IVANE JAVAKHISHVILI TBILISI STATE UNIVERSITY
ILIA VEKUA INSTITUTE OF APPLIED MATHEMATICS
GEORGIAN ACADEMY OF NATURAL SCIENCES

TBILISI INTERNATIONAL CENTRE OF
MATHEMATICS AND INFORMATICS

L E C T U R E N O T E S

of

T I C M I

Volume 15, 2014

Wolfgang H. Müller & Paul Lofink

THE MOVEMENT OF THE EARTH: MODELLING THE FLATTENING PARAMETER

Tbilisi

LECTURE NOTES OF TICMI

Lecture Notes of TICMI publishes peer-reviewed texts of courses given at Advanced Courses and Workshops organized by TICMI (Tbilisi International Center of Mathematics and Informatics). The advanced courses cover the entire field of mathematics (especially of its applications to mechanics and natural sciences) and from informatics which are of interest to postgraduate and PhD students and young scientists.

Editor: G. Jaiani
I. Vekua Institute of Applied Mathematics
Tbilisi State University
2, University St., Tbilisi 0186, Georgia
Tel.: (+995 32) 218 90 98
e.mail: george.jaiani@viam.sci.tsu.ge

International Scientific Committee of TICMI:
Alice Fialowski, Budapest, Institute of Mathematics, Pazmany Peter setany 1/C
Pedro Freitas, Lisbon, University of Lisbon
George Jaiani (Chairman), Tbilisi, I.Vekua Institute of Applied Mathematics, Iv. Javakhishvili Tbilisi State University
Vaxtang Kvaratskhelia, Tbilisi, N. Muskhelishvili Institute of Computational Mathematics
Olga Gil-Medrano, Valencia, Universidad de Valencia
Alexander Meskhi, Tbilisi, A. Razmadze Mathematical Institute, Tbilisi State University
David Natroshvili, Tbilisi, Georgian Technical University

Managing Editor: N. Chinchaladze

English Editor: Ts. Gabeskiria

Technical editorial board: M. Tevdoradze
M. Sharikadze

Cover Designer: N. Ebralidze

Abstracted/Indexed in: Mathematical Reviews, Zentralblatt Math

Websites: http://www.viam.science.tsu.ge/others/ticmi/lnt/lecturen.htm
http://www.emis.de/journals/TICMI/lnt/lecturen.htm

© TBILISI UNIVERSITY PRESS, 2014

Contents

Abstract. When modelling the motion of the Earth's axis, the so-called flattening is a crucial parameter. We define the term "flattening" as the difference between the equatorial and polar radii of the Earth normalized by the equatorial radius. It can either be measured or predicted by means of suitable models for the spinning Earth.

Newton was probably the first who suggested modelling the Earth as a liquid sphere, which during stationary spinning assumes the shape of an ellipsoid. However, in his famous Principia [1] he describes his method only verbally. Chandrasekhar [2] attempts to explain Newton's ideas in modern mathematical language and points out the various approximations. Modern fluid mechanics textbooks elaborate on this problem in their sections on rotational hydrodynamics, *e.g.*, [3].

Alternatively to the fluid model the rotating Earth can be modeled as a Hookean solid. Thomson and Tait [4] were seemingly the first to report corresponding results, albeit in a rather archaic notation of linear elasticity. Finally, Klein and Sommerfeld compiled results from both models in their treatise [5].

In this paper we will first give a critical overview of the historical development regarding the modelling of Earth's flattening. The next section contains a complete, modern treatment of the fluid model, and its application not only to the Earth but also to other celestial bodies. We will compare the results to actual measurements and discuss reasons for discrepancies. The next section deals with the Hookean model of the Earth, which we will also state and solve in modern terminology. In particular, we will not only compute the flattening but also present a complete solution for the stresses in a gravitating and stationary spinning, linear-elastic sphere. We will discuss possible extensions of the models, such as a Hookean hollow sphere with a liquid core, or even more complicated onion-layered type of models. The last section presents global balance arguments, by means of which information about the development and the final state of a spinning body can be obtained. In particular, we will investigate the work required for the spinning and for the subsequent deformation.

2000 Mathematical Subject Classification: 01-00, 31-00, 74-B05, 76-B07, 83-03 **Key words and phrases:** Flattening, fluid *vs.* Hookean model of Earth, stresses in celestial bodies

Wolfgang H. Müller* **and Paul Lofink**
Technische Universität Berlin, Institut für Mechanik, LKM
Einsteinufer 5,13591 Berlin, Germany

* Corresponding author. Email: wolfgang.h.mueller@tu-berlin.de

1 Some historical background and the experimental evidence

The rotation of matter gives rise to centrifugal accelerations, which, in turn, lead to its motion and, in addition, to its deformation. In particular, if the matter is a liquid these deformations may be considerable. Indeed, it was the great Newton who described in words in his famous bucket experiment in [1], pg. 51 the formation of what we now know to be a parabolic free water surface: "... recedet ipsa (*i.e.*, the water) paulatim a medio, ascendetque ad latera vasis, figuram concavam induens, (ut ipse expertus sum) ...." Note that his description is purely qualitative as well as heuristic, namely based on experience, as he says himself, despite the fact that he had developed calculus and was most likely in a position to predict the shape of the free surface mathematically. However, at least not in his Principia, no further quantification of the shape is attempted. This is different in the case of the figure of the Earth and other planets (he specifically mentions ***Jupiter***, showing a huge flattening that could easily be observed even in the old days, as well as the ***Earth***), which he idealizes as fluid bodies. Newton says in [1], pp. 592: "Planetae sublato omni motu circulari diurno figuram sphaericam, ob aequalem undique partium gravitatem, affectare deberent. Per motom illum circularem sit ut parte sab axe recedentes juxta aequatorum ascendere conentur. Ideoque material si ***fluida*** sit ascensu suo ad aequatorem diametros adaugebit, axem vero sescensu suo ad polos diminuet. Sic ***jovis*** diameter (consentientibus astronomorum observationibus) brevior deprehenditur inter polos quam ab oriente in occidentem. Eodem argumento, nisi ***terra*** nostra paulo altior esset sub aequatore quam ad polos, maria ad polos subsiderent, & juxta aequatorem ascendendo, ibi omnia inundarent." The latter is obviously a gut feeling statement of Newton, the discoverer of the law of gravity, as we shall see shortly. However, the rest of the passage anticipates the mathematical definition of the *flattening* or *ellipticity*, f, which is given by the following ratio [6], Chapter 6:

$$f = \frac{a - c}{a}. \tag{1.1}$$

a denotes the (mean) equatorial radius and c the polar radius of the celestial body. In contrast to the bucket problem Newton quantifies the flattening of the Earth, first, based on geodesic experiments of his time, *cf.*, pp. 593 of [1]. Second, he conceives a rather strange fluid model of the Earth, which Chandrasekhar [2], pp. 384 has termed ***the method of the canals***: Two straight canals, one along the equatorial and one along the polar axis of the Earth, are filled with water and interconnected at a right angle. Newton considers stationary conditions and equilibrium of forces resulting from gravity and centrifugal acceleration. However, he does not really detail the mathematical analysis. Rather he explains his findings with many words: Section 414 of [1], pp. 596. Luckily, Chandrasekhar translates Newton's thoughts for

us less gifted. For small values of f we may write:

$$f = \frac{5}{4}\frac{a\omega_0^2}{Gm/a^2} \equiv \frac{5}{4}\frac{\omega_0^2 a^3}{Gm}, \tag{1.2}$$

where $G = 6.673 \cdot 10^{-11}\,\frac{\mathrm{m}^3}{\mathrm{kgs}^2}$ stands for the gravitational constant, m is the mass of the celestial body, and ω_0 is its (constant) angular velocity. Thus, we may say that the flattening is basically given by the ratio of angular acceleration to gravitational acceleration, and the ominous factor 5/4 accounts for the difference between the gravitational acceleration at the pole and at the equator, which follows from the specific weights of the two water columns in an oblate spheroid.

It is more than fair to say that Newton withheld all the details explaining how his law of gravity might have led to this result (Chandrasekhar surmises for good reasons that Newton must have known the formulae for the gravitational attraction of an oblate spheroid). Of course, Newton does also not provide a concise formula for the flattening, such as the one above. Rather his approach is a mix of (hidden) theory and experimental evidence. For example, he uses experimental results for the gravitational plus the centrifugal acceleration in Paris to make conclusions regarding the situation at the equator's surface, *e.g.*, "Et vis tota gravitatis in latitudine illa (*i.e.*, Paris) erit at vim centrifugam corpore in aequatore terrae ut 2177,267 ad 7,54064 seu 289 ad 1." [1], pg. 596. This in mind he then turns back to his gedanken experiment of the two interconnected canals and concludes after a long line of arguments involving equilibrium of forces and his law of gravity: "Et altitudo ejus ad aequatorem erit 19658600 pedum circiter, & ad polos 19573000 pedum." [1], pg. 598.

Chandrasekhar presents a translation of Newton's line of thoughts on pp. 389 of [2] together with many annotations. We leave it to the reader to ponder over the details and only conclude that Newton's predicted value for the flattening of a homogeneous Earth is $f_{\mathrm{E}} = 4.35 \cdot 10^{-3}$. Furthermore, if we take Eqn. (1.2) for granted and insert the following currently accepted values for the mass of the Earth, $m_{\mathrm{E}} = 5.972 \cdot 10^{24}\mathrm{kg}$, its equatorial radius, $a_{\mathrm{E}} = 6.378 \cdot 10^{6}\mathrm{m}$, and its angular (sidereal) speed $\omega_{0,\mathrm{E}} = 2\pi/86,164\ \mathrm{s}$ [7] we find that $f_{\mathrm{E}} = 4.33 \cdot 10^{-3}$. Indeed, this is amazingly close to Newton's figure. However, modern sources quote a different number for the observed flattening of the Earth, *e.g.*, NASA's [8] $f_{\mathrm{E}} = 3.35 \cdot 10^{-3}$.

There are several reasons for the discrepancy. As we shall see below, one of the main factors is the assumption of a fluid model, which forms the basis of Eqn. (1.2). Moreover, in the same context the following remark is in order: Frequently it remains unclear as to whether a quoted number for the flattening truly results from direct length measurements or from some model equation. In other words, circular conclusions are immanent. We will comment on this issue even more later.

It is worth mentioning that Newton also applies his fluid model to explain the rather large flattening value, f_{J}, for Jupiter. For this purpose, he reinter-

prets Eqn. (1.2) in terms of (homogeneous) mass densities, ρ, so to speak:

$$f = \frac{3}{4\pi}\frac{\omega_0^2}{G\rho} \quad \Rightarrow \quad f_{\mathrm{J}} = f_{\mathrm{E}} \left(\frac{\omega_{0,\,\mathrm{J}}}{\omega_{0,\mathrm{E}}}\right)^2 \frac{\rho_{\mathrm{E}}}{\rho_{\mathrm{J}}}. \tag{1.3}$$

Newton had some information on the relative densities of celestial bodies based on his gravitational law, the measured times of revolution, and the distances of the moons orbiting around them: "Erant autem verae solis, jovis, saturni ac terrae diametri ad invicem ut 10000, 997, 791, & 109, ... & propterea densitates sunt ut 100, 94, 67 & 400." (Liber III, Propositio VIII, Theorema VIII, Corol. 3 in [1], pg. 582). He concludes: "... sintque temporum quadrata ut 29 ad 5, & revolventium densitates ut 400 ad $94\frac{1}{2}$ (*n.b.*, Eqn. $(3)_2$) ... Est igitur diameter iovis ab oriente in occidentem ducta, ad ejus diametrum inter polos ut $10\frac{1}{3}$ ad $9\frac{1}{3}$ quamproxime." [1], pg. 599. We conclude that $f_{\mathrm{J}} = 9.68 \cdot 10^{-2}$. However, the modern figure reported by NASA is $f_{\mathrm{J}} = 6.49 \cdot 10^{-2}$ [8]. It is curious to note that in both cases, for the Earth as well as for Jupiter, the predicted flattening value is higher than the actually observed one. We will get back to this issue later.

We now turn to the historical development of solid mechanics models for the flattening. First, an answer to the question, why we need such models to begin with, seems necessary. To that end, we simply cite from [5], pg. 687: "... the assumption of a fluid interior in a compliant shell is refuted by the phenomenon of the tides. A thin crust of the Earth with the elastic compliability of the materials known to us would follow the deforming influence of the tidal forces almost as willingly as the water of the sea. There would then be, however, no relative motion of the water with respect to the land under the influence of these forces, but only a common rise and fall of the sea and the continents that would escape immediate perception. Thus there remains only the assumption that the Earth is, in the mean, effectively solid ... ."

Thus, the emphasis is on ***tidal effects***. Consequently, it is not surprising that the flattening problem is frequently discussed in context with the more general question of how the Earth deforms, if it is subjected not only to its own gravitational field and to centrifugal accelerations, but also to the gravitational influence of external celestial bodies, such as the Moon and the Sun.

Note that traditionally we refer to "tides" when we think of the rise and fall of sea levels, dictated by the Moon's or the Sun's periodic gravitational pull. However, geologists and astrophysicists have a much wider notion of this word. To them it means, quite general, any permanent or periodic movement of the surface of the Earth, water or land, resulting from internal or external forces.

Today we would say that if we wish to model the deformation of the Earth when subjected to forces we need an appropriate constitutive model. In particular, if we want to emphasize Earth's solid characteristics we need constitutive models pertinent to solids. Clearly, the concept of constitutive equations was in its infancy when this need arose first and, hence, Sommerfeld explains to us

in great detail on pg. 685 in [5] that the transition between a fluid and a solid can be gradual. In fact, the only constitutive law available in the middle of the nineteenth century that had a sound mathematical basis and could therefore be used to study three-dimensional continua was Hooke's law of linear elasticity. However, it is fair to say that tensor notation was still under development at that time and the few papers dedicated to the problem of a sphere subjected to general gravitation, *i.e.*, tides, and centrifugal forces are written in a most repelling notation. In Section 3 we will revisit the problem in modern form. Thus, at this point it may suffice to mention that, at least to our knowledge, the first source that presents an explicit formula for the flattening of a rotating, self-gravitating, compressible, linear-elastic sphere is Thomson and Tait's treatise [4], pg. 432, which in modern notation reads

$$f = \frac{\rho_0 R^2 \omega_0^2}{E} \frac{(1+\nu)\,(2+\nu)}{7+5\nu}. \tag{1.4}$$

E denotes Young's modulus, ν is Poisson's ratio, ρ_0 and R are the mass density and the radius of the sphere in its reference configuration, respectively. Of course, the question arises which elastic constants to use for the Earth. If we take the ones for steel, as suggested in [5], pp. 692, *i.e.*, $E_{\mathrm{E}} \approx 210$ GPa, and $\nu_{\mathrm{E}} \approx 0.3$, we find with $\rho_{0,\mathrm{E}} \approx 5,514 \frac{\mathrm{kg}}{\mathrm{m}^3}$, $R_{\mathrm{E}} = 6.371 \cdot 10^6 \mathrm{m}$, the mean radius of the Earth [7], a value of $f_{\mathrm{E}} = 2 \cdot 10^{-3}$, and we may conclude that a solid Earth model leads to an underestimate of the observed figure. In fact, we shall see later that the question which radius and which Young's modulus to use is rather subtle and difficult to answer. However, for the time being, we may say that the Earth is somewhere in between a fluid and a (linear-elastic) solid.

2 A fluid model for the flattening

2.1 Theory

Recall the Euclidian transformation $\boldsymbol{x}' = \boldsymbol{x} + \boldsymbol{b}$ between an inertial system and a non-inertial frame (identifiable by the dash with the Cartesian unit base $\boldsymbol{e}'_i$). The origins of the two systems are separated by the vector $\boldsymbol{b}$. We may write for the relations between the velocities and the accelerations in both systems (see, *e.g.*, [9], pp. 183):

$$\begin{aligned} \boldsymbol{x}' = \boldsymbol{x} + \boldsymbol{b} \quad \Rightarrow \quad \boldsymbol{v}' = \boldsymbol{v} - \boldsymbol{\omega} \times \boldsymbol{x}' + \dot{\boldsymbol{b}} \quad \Rightarrow \\ \boldsymbol{a}' = \boldsymbol{a} - 2\boldsymbol{\omega} \times \boldsymbol{v}' - \boldsymbol{\omega} \times (\boldsymbol{\omega} \times \boldsymbol{x}') - \dot{\boldsymbol{\omega}} \times \boldsymbol{x}' + \ddot{\boldsymbol{b}}. \end{aligned} \tag{2.1}$$

Thus the balance of momentum for the non-inertial system reads (see, *e.g.*, [9], pg. 199):

$$\rho \frac{\mathrm{d}\boldsymbol{v}'}{\mathrm{d}t} = \nabla' \cdot \boldsymbol{\sigma} + \rho \left(\boldsymbol{f} - 2\boldsymbol{\omega} \times \boldsymbol{v}' - \boldsymbol{\omega} \times (\boldsymbol{\omega} \times \boldsymbol{x}') - \dot{\boldsymbol{\omega}} \times \boldsymbol{x}' + \ddot{\boldsymbol{b}} \right). \tag{2.2}$$

The Earth rotates at a constant angular speed, *i.e.*, $\dot{\boldsymbol{\omega}} = \boldsymbol{0}$, and we assume stationary conditions, *i.e.*, $\boldsymbol{v}' = \boldsymbol{0}$. Moreover, the origins of the two systems shall coincide, *i.e.*, $\boldsymbol{b} = \boldsymbol{0}$. Consequently:

$$\nabla' \cdot \boldsymbol{\sigma} + \rho \left(\boldsymbol{f} - \boldsymbol{\omega} \times (\boldsymbol{\omega} \times \boldsymbol{x}') \right) = \boldsymbol{0}. \tag{2.3}$$

For a fluid at rest (w.r.t. the non-inertial frame) the stress tensor reduces to an isotropic pressure, *i.e.*, $\boldsymbol{\sigma} = -p\boldsymbol{1}$. Moreover, potentials can be used to obtain the gravitational as well as the centrifugal acceleration by differentiation w.r.t. position, *i.e.*, $\boldsymbol{f} = -\nabla' U^f$ and $-\boldsymbol{\omega} \times (\boldsymbol{\omega} \times \boldsymbol{x}') = -\nabla' U^\omega$. Finally we assume incompressibility, *i.e.*, $\rho = \rho_0 = \text{const.}$, and therefore:

$$\nabla' \left[p + \rho_0 \left(U^f + U^\omega \right) \right] = \boldsymbol{0}. \tag{2.4}$$

We use Cartesian coordinates in the non-inertial frame (*i.e.*, commoving ones, which explains the dash), such that $\boldsymbol{\omega} = \omega' \ \boldsymbol{e}'_3 = \omega_0 \ \boldsymbol{e}'_3$, $\omega_0 = \text{const.}$, and consequently:

$$\begin{aligned} &-\nabla' U^\omega = -\boldsymbol{\omega} \times (\boldsymbol{\omega} \times \boldsymbol{x}') = \omega_0^2 \ (x'_1 \boldsymbol{e}'_1 + x'_2 \boldsymbol{e}'_2) \\ &\Rightarrow \ U^\omega = -\tfrac{1}{2}\omega_0^2 \left(x_1'^2 + x_2'^2 \right). \end{aligned} \tag{2.5}$$

In general, we may write for the gravitational potential at a point $\boldsymbol{x}'$ within an inhomogeneous material region $\tilde{V}$ (see [10], pg. 170):

$$U^f (\boldsymbol{x}') = -G \int_{\tilde{V}} \frac{\rho(\tilde{\boldsymbol{x}}) \, \mathrm{d}\tilde{V}}{|\boldsymbol{x}' - \tilde{\boldsymbol{x}}|}. \tag{2.6}$$

In order to solve the integral we have to specify the mass density within the body as well as its shape. For the case of a homogeneous ellipsoid with three

different principal axes, a_i, (a.k.a. Maclaurin ellipsoid in geodesy) the 3D integration can be reduced to one-dimensional integrals, *cf.*, [3], pg. 45 (note that Einstein's summation rule applies; m denotes the total mass of the ellipsoid):

$$U^f\left(\boldsymbol{x}'\right) = -\tfrac{3}{4}Gm\left(\alpha_0 - \alpha_i x_i'^2\right) \equiv -\pi G\rho_0 a_1 a_2 a_3\left(\alpha_0 - \alpha_i x_i'^2\right), \tag{2.7}$$

$$\alpha_0 = \int_0^\infty \frac{\mathrm{d}u}{\Delta}, \alpha_i = \int_0^\infty \frac{\mathrm{d}u}{\left(a_i^2+u\right)\Delta}, \Delta = \left(a_1^2+u\right)^{\frac{1}{2}}\left(a_2^2+u\right)^{\frac{1}{2}}\left(a_3^2+u\right)^{\frac{1}{2}}.$$

It is fair to say that with this equation we anticipate the equilibrium shape of the spinning Earth as a spheroid, *i.e.*, an ellipsoid with, in the end, two principal axes of equal length. Be that as it may, but Eqn. (2.4) can now be integrated, and the result is:

$$p\left(\boldsymbol{x}'\right) = \\ p\left(\mathbf{0}\right) - \tfrac{1}{2}\rho_0\left[\left(\tfrac{3}{2}Gm\alpha_1 - \omega_0^2\right)\ x_1'^2 + \left(\tfrac{3}{2}Gm\alpha_2 - \omega_0^2\right)\ x_2'^2 + \tfrac{3}{2}Gm\alpha_3 x_3'^2\right]. \tag{2.8}$$

This equation is not very useful yet, for several reasons. First, the central pressure $p\left(\mathbf{0}\right)$ is not known. Second, the lengths, a_i, of the principal axes are not known either. In fact, we would like to predict their size as functions of the mass of the spheroid, its angular speed, etc. In order to carry things forward we concentrate on the outer periphery of the ellipsoid, which is described by the equation:

$$\frac{X_1'^2}{a_1^2} + \frac{X_2'^2}{a_2^2} + \frac{X_3'^2}{a_3^2} = 1. \tag{2.9}$$

Note that we identify periphery locations by the vector $\boldsymbol{X}'$. Moreover, we assume that the atmospheric pressure acting on the Earth's surface can be neglected and put it equal to zero. Therefore, Eqn. (2.8) leads to:

$$\frac{X_1'^2}{\left(\alpha_1 - \frac{\omega_0^2}{\frac{3}{2}Gm}\right)^{-1}\frac{4p(\mathbf{0})}{3\rho_0 Gm}} + \frac{X_2'^2}{\left(\alpha_2 - \frac{\omega_0^2}{\frac{3}{2}Gm}\right)^{-1}\frac{4p(\mathbf{0})}{3\rho_0 Gm}} + \frac{X_3'^2}{\alpha_3^{-1}\frac{4p(\mathbf{0})}{3\rho_0 Gm}} = 1, \tag{2.10}$$

due to the requirement of continuity of the tractions of a surface at rest (w.r.t. the non-inertial frame). Eqn.'s (2.9) and (2.10) must be satisfied simultaneously, and therefore:

$$\frac{4p\left(\mathbf{0}\right)}{3\rho_0 Gm} = \left(\alpha_1 - \frac{\omega_0^2}{\frac{3}{2}Gm}\right)a_1^2 = \left(\alpha_2 - \frac{\omega_0^2}{\frac{3}{2}Gm}\right)a_2^2 = \alpha_3 a_3^2. \tag{2.11}$$

This leads after some algebraic manipulations to:

$$\left(a_2^2 - a_1^2\right)\int_0^\infty \left[\frac{a_1^2 a_2^2}{\left(a_1^2+u\right)\left(a_2^2+u\right)} - \frac{a_3^2}{\left(a_3^2+u\right)}\right]\frac{\mathrm{d}u}{\Delta} = 0, \tag{2.12}$$

which leads us to conclude that the ellipsoid must be a spheroid, *i.e.*, $a_1 = a_2 \equiv a$, as might be expected due to the rotation about a fixed axis and isotropy of

space. So far the mathematical model. It is interesting to note that there is experimental evidence, which shows that this is only approximately true. Bretagnon *et al.* report in [11] or Bursa in [12] that ***three*** principal moments of inertia are required to describe the observed precession rate of the Earth more accurately: $I_{11} \equiv A = 0.329611083 \cdot m_{\mathrm{E}} a_{\mathrm{E}}^2$, $I_{22} \equiv B = 0.329618344 \cdot m_{\mathrm{E}} a_{\mathrm{E}}^2$, and $I_{33} \equiv C = 0.330697340 \cdot m_E a_{\mathrm{E}}^2$. We conclude that the resistance to rotation about the polar axis is greatest, whereas resistance to rotation about the two equatorial principal axes is smaller and almost equal. Almost! B is slightly larger than A. If we assume a homogeneous ellipsoid, such that $A = \frac{1}{5} m_{\mathrm{E}} \left(b_{\mathrm{E}}^2 + c_{\mathrm{E}}^2\right)$ and $B = \frac{1}{5} m_{\mathrm{E}} \left(a_{\mathrm{E}}^2 + c_{\mathrm{E}}^2\right)$, we conclude that a_{E} should be slightly larger than b_{E}. However, for a homogeneous Earth ellipsoid we should also have $a_{\mathrm{E}} = \sqrt{\frac{5}{2m_{\mathrm{E}}} (B + C - A)}$, a relation, which is ***not*** guaranteed by the numbers shown above. The reason is very simple: The Earth is inhomogeneous. Its core is much denser than the outside regions and this has an influence on its precession rate, a figure that was used to compute the numerical values for the principal moments of inertia. Thus, as common to all models, our simple assumption of a fluid, spheroidal Earth has its limits. It is worth pointing out that the earlier literature ignored differences between A and B due to insufficient accuracy of measurements at that time, see, *e.g.*, [13]. It is also worth commenting that our implicit assumption according to which the principal axes of the real Earth point in the direction of the Earth's geographical pole and its equatorial regions is an approximation. Moreover, the polar or rather the third principal axis of the real Earth does not perfectly coincide with the direction of the angular velocity vector, a phenomenon, which is known as the Earth's wobble. All of this underlines the limits of the assumption of a perfectly symmetric spheroid rotating about its polar axis.

On the other hand we obtain from Eqn. (2.11):

$$\frac{2\omega_0^2 a^3}{3Gm} = \frac{(1 + 2\lambda^2) \arccos\lambda - 3\lambda\sqrt{1 - \lambda^2}}{(1 - \lambda^2)^{3/2}}\,, \quad \lambda = \frac{a_3}{a_1} \equiv \frac{c}{a}. \tag{2.13}$$

because the following integrals can now be solved in closed form:

$$\alpha_0 = \frac{1}{a} \int_0^\infty \frac{\mathrm{d}\upsilon}{(1 + \upsilon)\left(\lambda^2 + \upsilon\right)^{1/2}} = \frac{2}{a} \frac{\arccos\lambda}{\sqrt{1 - \lambda^2}}\,, \quad \upsilon = \frac{u}{a^2}.$$

$$\alpha_1 \equiv \alpha_2 = \frac{1}{a^3} \int_0^\infty \frac{\mathrm{d}\upsilon}{(1 + \upsilon)^2 \left(\lambda^2 + \upsilon\right)^{1/2}} = \frac{1}{a^3} \frac{\lambda}{1 - \lambda^2} \left[\frac{\arccos\lambda}{\lambda\sqrt{1 - \lambda^2}} - 1\right], \tag{2.14}$$

$$\alpha_3 = \frac{1}{a^3} \int_0^\infty \frac{\mathrm{d}\upsilon}{(1 + \upsilon)\ \left(\lambda^2 + \upsilon\right)^{3/2}} = \frac{1}{a^3} \frac{2\left(\sqrt{1 - \lambda^2} - \lambda \arccos\lambda\right)}{\lambda \left(1 - \lambda^2\right)^{3/2}}.$$

An alternative but numerically equivalent solution in terms of $\arcsin\lambda$ was presented in [3], pg. 46. For a given angular velocity Eqn. (2.13) allows to

calculate the flattening of a body of mass m and equatorial radius a_1 numerically. For this purpose note that $f = 1 - \lambda$. Moreover, we can expand Eqn. (2.13) in a series for the flattening:

$$\frac{2\omega_0^2 a^3}{3Gm} = \frac{8}{15} f + \frac{44}{105} f^2 + \mathrm{O}\left[f\right]^3 . \tag{2.15}$$

Obviously, the first term is dominant for small flattening values and agrees with Newton's result from Eqn. (1.2). It is curious to note that Maclaurin was obviously the first who presented a solution to the flattening problem in terms of a series about $f \approx 0$ (which in hindsight explains the term Maclaurin series, *i.e.*, a series close to the point zero). In Section 655 of the first volume of his book on fluxions [14], pp. 543 we find: "The gravity ... represented ... at the equator by D, and the centrifugal force at D by V, ..., if the density of the spheroid be uniform ... the ratio of V to D may be determined to any degree of exactness, at pleasure. ... the excess of the semidiameter of the equator above the semiaxis is to the mean semidiameter nearly as 5V to 4D $-$ $\frac{11\mathrm{V}}{7}$." Now, Eqn. (2.7) allows us to calculate the magnitude of gravitational acceleration at the equator of a spheroid:

$$\mathrm{D} = \frac{3Gm}{2a_1^2} \frac{1}{1-\lambda^2} \left[\frac{\arccos \lambda}{\sqrt{1-\lambda^2}} - \lambda \right] . \tag{2.16}$$

And since the centrifugal acceleration at the equator of the spheroid is given by $\mathrm{V} = a\omega_0^2$, a series expansion leads to:

$$\frac{2\omega_0^2 a^3}{3Gm} = \frac{\frac{4}{5} f}{1 + \frac{44}{35} f} \frac{1}{1-\lambda^2} \left[\frac{\arccos \lambda}{\sqrt{1-\lambda^2}} - \lambda \right] = \frac{8}{15} f - \frac{184}{525} f^2 + \mathrm{O}\left[f\right]^3 , \tag{2.17}$$

if we accept the quoted result from Maclaurin's book. In comparison with Eqn. (2.15) we conclude that the dominant (*i.e.*, Newton's) term comes out correctly, the higher order terms, however, do not. In fact, Maclaurin never claimed this to be the case, and it is fair to say that a closed form solution, such as Eqn. (2.13), does not appear in his treatise, as one could surmise from a remark on pg. 47 of [3].

We will now turn to Eqn. (2.8) and compute the pressure function $p\left(\boldsymbol{x}'\right)$. This will later put us in a position to compare the result to expressions for the Hookean stresses. It is advisable to use generalized, co-moving, spherical coordinates [15] as follows:

$$\begin{aligned} x_1' = a\ \xi_1 \cos\xi_2 \sin\xi_3, x_2' = a\ \xi_1 \sin\xi_2 \sin\xi_3, x_3' = c\ \xi_1 \cos\xi_3, \\ \xi_1 \in \left[0,1\right], \xi_2 \in \left[0, 2\pi\right], \xi_3 \in \left[0,\pi\right] . \end{aligned} \tag{2.18}$$

It is now a matter of straightforward algebra to derive the following result by combining Eqn.'s (2.8), (2.11), and (2.14):

$$\begin{aligned} p\left(\xi_1\right) &= p\left(\mathbf{0}\right)\ \left(1 - \xi_1^2\right) , \\ p\left(\mathbf{0}\right) &= \frac{3\rho_0 Gm}{2a} \left(1 - \frac{\lambda}{\sqrt{1-\lambda^2}} \arccos\lambda \right) \frac{\lambda}{1-\lambda^2} . \end{aligned} \tag{2.19}$$

Note that for vanishing flattening, *i.e.*, $\lambda = 1$ we have:

$$p(\xi_1) = \frac{\rho_0 G m}{2R}\left(1 - \xi_1^2\right). \tag{2.20}$$

In fact, this corresponds equation-wise to the result for the pressure distribution in a self-gravitating, non-rotating, homogeneous sphere of radius $a = c \equiv R$: Recall that the gravitational acceleration at a radial position within such a sphere is given by $\boldsymbol{f} = -Gm(r)/r^2 \boldsymbol{e}_r$ where $m(r) = \frac{4\pi}{3}\rho_0 r^3$ is the total mass "beneath" that position (*cf.*, [9], pp. 269). Thus from the analogue to Eqn. (2.2) in the inertial frame we conclude that:

$$\nabla \cdot \boldsymbol{\sigma} = -\rho\, \boldsymbol{f} \quad \Rightarrow \quad p(r) = -\tfrac{1}{2}\tfrac{4\pi}{3} G \rho_0^2 r^2 + C. \tag{2.21}$$

The constant of integration is determined by the requirement of vanishing pressure at the outer surface of the sphere at the outmost radial position, R. Hence:

$$p(r) = \frac{\rho_0 G m}{2R}\left(1 - \frac{r^2}{R^2}\right), m = \tfrac{4\pi}{3}\rho_0 R^3. \tag{2.22}$$

In comparison with Eqn. (2.20) we may interpret the generalized spherical coordinate as a normalized measure of the radial distance from the center of the ellipsoid to an arbitrary point within. We may also be tempted to conclude that because Eqns. (2.20/22) refer to pressure induced ***exclusively*** by gravitation, Eqn. (2.19) includes only gravitational but no centrifugal effects. Moreover, the angular velocity ω_0 does not occur in this expression at all. This conclusion, however, is erroneous: Alternatively, Eqn. (2.11) allows us by using Eqn. $(2.14)_2$ to write for $p(\mathbf{0})$ in Eqn. (2.19):

$$p(\mathbf{0}) = \frac{3\rho_0 G m}{4a}\left(\frac{1}{\lambda\sqrt{1-\lambda^2}}\arccos\lambda - 1\right)\frac{\lambda}{1-\lambda^2} - \tfrac{1}{2}\rho_0\omega_0^2 a^2. \tag{2.23}$$

The first term is always positive and accounts for gravitational effects only. The second one is clearly negative and shows that the centrifugal acceleration leads to a pressure decrease. Moreover, if we insert Eqn. (2.13) into (2.23), we reobtain Eqn. (2.19). This proves that $p(\mathbf{0})$ of Eqn. (2.19) is truly the net pressure. Moreover, note that the pressure vanishes everywhere, provided $\lambda = 0$, *i.e.*, in the case of total flattening, $f = 1$. Then according to Eqn. (2.13) the corresponding, critical angular velocity is given by $\omega_0^c = \pi\sqrt{G\rho_0}$. For a liquid Earth this would result in a revolution time of ca. 3300 seconds. This is, of course, just a curious, totally unrealistic result.

Table 1: Experimentally observed and predicted flattening values.

	ω_0 [1/s]	a_1 [m]	m [kg]	f (Newton)	f (exact)	f [8,16]
Planets						
Mercury	1.23993E-06	2.4395E+06	3.300E+23	1.26683E-06	0.0E+00	0.000E+00
Venus	-2.99242E-07	6.0520E+06	4.870E+24	7.63391E-08	0.0E+00	0.000E+00
Earth	7.30263E-05	6.3780E+06	5.970E+24	4.34083E-03	4.32631E-03	3.350E-03
Mars	7.09483E-05	3.3960E+06	6.420E+23	5.75157E-03	5.72576E-03	5.890E-03
Jupiter	1.76296E-04	7.1492E+07	1.898E+27	1.12071E-01	1.03131E-01	6.487E-02
Saturn	1.63115E-04	6.0268E+07	5.680E+26	1.92058E-01	1.67431E-01	9.796E-02
Uranus	-1.01473E-04	2.5559E+07	8.680E+25	3.70974E-02	3.60525E-02	2.293E-02
Neptune	1.08406E-04	2.4764E+07	1.020E+26	3.27717E-02	3.19531E-02	1.708E-02
Pluto	-1.13851E-05	1.1950E+06	1.310E+22	3.16255E-04	3.16178E-04	0.000E+00
Stars						
Sun	2.86533E-06	6.96342E+08	1.9886E+30	2.61105E-05	2.61139E-05	5.000E-05
Achernar	3.49445E-05	8.35610E+09	1.3323E+31	1.00160E+00	5.83710E-01	3.103E-01
Regulus	1.09432E-04	2.89678E+09	7.5565E+30	7.21520E-01	4.72896E-01	2.453E-01
Vega	1.39475E-04	1.93583E+09	4.2456E+30	6.22579E-01	4.27247E-01	1.870E-01
Alderamin	1.44117E-04	1.96368E+09	3.7782E+30	7.79630E-01	4.97959E-01	2.296E-01
Altair	1.87638E-04	1.47625E+09	3.5595E+30	5.96023E-01	4.14304E-01	1.916E-01

2.2 Evaluation and comparison to observations

The basis of Table 1 are experimental data compiled in [8] and [16], pg. 179. They were used to obtain predictions for the flattening of various celestial bodies. f (Newton) refers to predictions that were made by using Newton's result shown in Eqn. (1.2). f (exact) is based on a numerical solution of Eqn. (2.13).

Figs. 2.1 and 2.2 allow for a direct comparison of the observed and the predicted values for the flattening of planets and stars in graphical form. The following conclusions can be drawn. Loosely speaking, one would expect that gassy bodies, such as the gas giants or stars, should follow the fluid model quite closely. However, independently of the planet or of the star, the fluid model tends to overestimate the flattening. In fact, Newton's formula leads to the highest overestimates. The numerical solution of Eqn. (2.13) predicts flattenings that are closer to the observed values. Note that in the case of Mars the predictions match reality surprisingly well. This is also true for Mercury and Venus. However, their flattening values are close to zero, anyway.

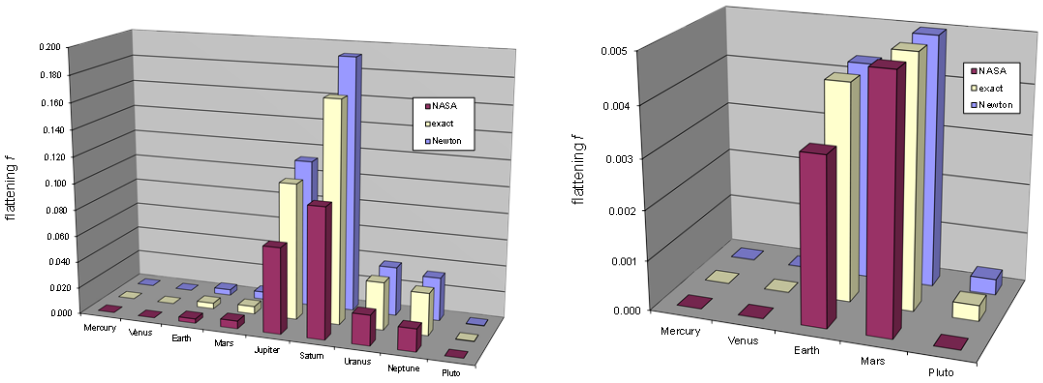

Fig. 2.1: Comparison of observed and predicted flattening values for the planets.

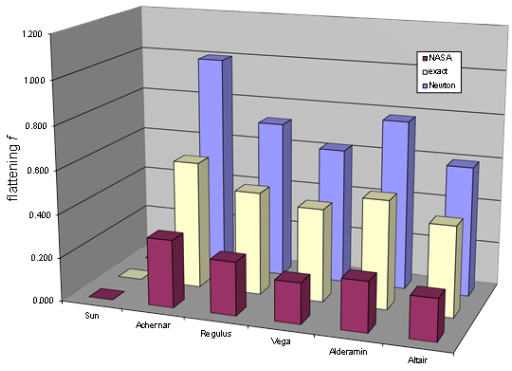

2.2: Comparison of observed and predicted flattening values for some stars.

One reason for the obvious discrepancy is the assumption of incompressibility, *i.e.*, a constant mass density ρ_0 throughout the body. However, this is not a very realistic assumption, since the mass density increases, if we approach the center of the celestial body. This is specified for the Earth in the PREM model [17], pg. 312, for gas giants like Jupiter or Saturn in [18], or for the Sun in [19], pp. 43. Within our fluid model there is no place for a radially varying density. However, the following simple argument shows in which direction the flattening will change if mass is accumulated closer to the center of an ellipsoidal fluid body rotating at a fixed angular speed. Suppose we compress the matter of an ellipsoid such that it occupies only half of the original equatorial radius. This will require its constant mass density to increase roughly by the factor of eight. According to Eqn. (1.2) this would lead to a decrease of the flattening by one eighth. We may thus suspect that rearranging matter of a fixed amount toward the center will have the same effect.

The flattening of our Moon deserves a separate comment. The observed value of 0.0012 [8] is small but distinct from zero. Of course we cannot simply apply Eqns. (1.2) or (2.13) since the Moon "is tidally coupled to the Earth so that the same side of the Moon always faces the Earth, the rotation of the Moon is too small to explain the observed value of J_2 [the moment of inertia, C]. However, the present flattening may be a relic of a time when the Moon was rotating more rapidly. At that time the lunar lithosphere may have thickened enough so that the strength of the elastic lithosphere was sufficient to preserve the rotational flattening." [20], pg. 377. We may now use Eqn. (2.13) and the data for mass and equatorial radius presented in [8] to predict that the former rotation rate of the Moon was roughly 58 h. Note that for the evaluation Fig. 2.3 is very useful.

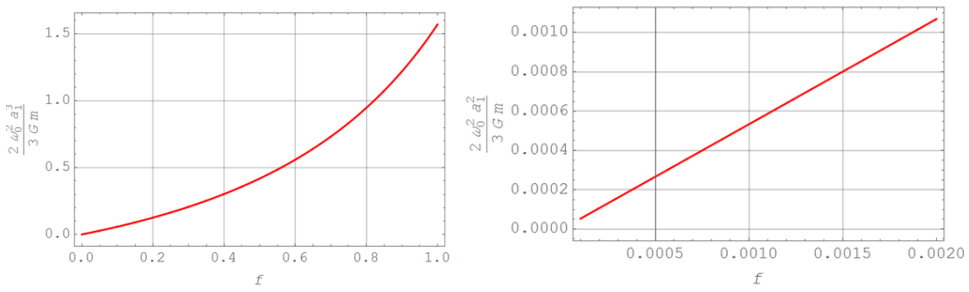

Fig. 2.3: Graphic representation of Eqn. (16), a means to correlate angular velocity with the predicted flattening.

The other big moons of our solar system, like Io [21], Europa [22], Ganymede [23], and Callisto [24] of Jupiter, or Titan of Saturn [25] show also tidal coupling to their planet. According to the literature they seem to have no or almost no flattening, or, like Io a strongly ellipsoidal shape, which cannot be explained by our axis-symmetric fluid model. The latter is also the case for large asteroids from the asteroid belt between Mars and Jupiter, which is why they are not studied here either.

We now discuss the evolution of the pressure as a function of quasi-radial distance, ξ_1, according to the incompressible fluid model. To this end we may start directly from Eqn. (2.19), which is plotted in Fig. 2.4 (black lines). The red lines stem from the so-called PREM model [17], which is based on experimental evidence (elastic wave scattering) and allows for compressibility.

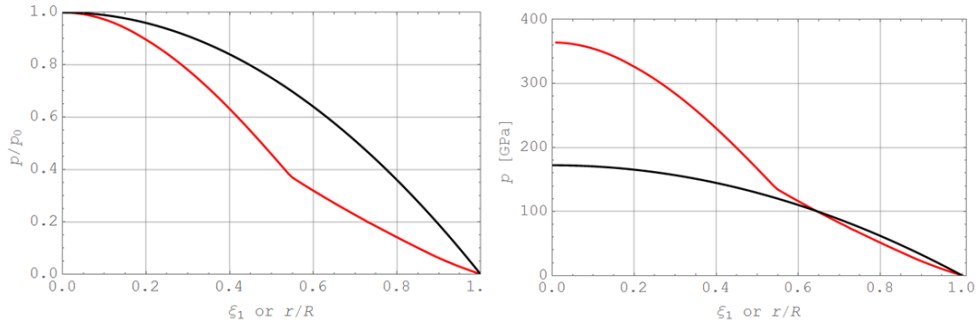

Fig. 2.4: Modelling the pressure distribution within the Earth as a function of dimensionless radius, ξ_1, using an incompressible fluid model (black) and the PREM model (red).

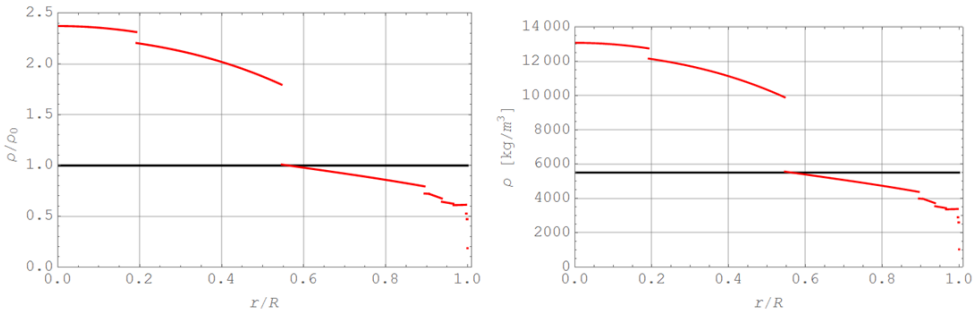

Fig. 2.5: Mass density distribution within the Earth as a function of dimensionless radius, r/R, according to the PREM model (red) in comparison with the average mass density, $\rho_0 = \rho\,(r=0)$.

Obviously there is a distinct transition point (the end of the outer core), where the pressure shows a kink when plotted over the dimensionless radius, r/R. In this context, it is fair to point out that the PREM model considers the Earth as spherical. The reason for the transition is the huge jump in mass density when entering the outer core, *i.e.*, essentially changing from the density of silicon dioxide to iron. The corresponding density plots are shown in Fig. 2.5.

In Table I of the PREM model [17] the mass density was fitted piecewise by splines, which is in agreement with the numerical data presented in the additional Table II. In the latter pressure data is also recorded. However, the pressure can be calculated as follows, once the density function $\rho = \rho\,(r/R)$ is known. We start from Poisson's equation for the gravitational potential in the inertial frame, specialized to the case of purely radial dependence:

$$\Delta U^f = 4\pi\rho\,(\boldsymbol{x}') \quad \Rightarrow \quad \frac{1}{r^2}\frac{\mathrm{d}}{\mathrm{d}r}\left(r^2\frac{\mathrm{d}U^f}{\mathrm{d}r}\right) = 4\pi\rho\,(r) \quad \Rightarrow \tag{2.24}$$

$$\frac{\mathrm{d}U^f}{\mathrm{d}r} = \frac{m\,(r)}{r^2} \quad \text{with} \quad m\,(r) = 4\pi\int_{\bar{r}=0}^{\bar{r}=r}\rho\,(\bar{r})\,\bar{r}^2\,\mathrm{d}\bar{r}.$$

This corresponds to the well-known fact that the gravitational attraction in a sphere of purely radially dependent density is given by Newton's law for point masses as if the mass $m\,(r)$ "beneath" the radial point of interest were concentrated at $r = 0$. We now turn to the local balance of momentum specialized to the stationary case for a fluid and to purely radial dependencies. Then this vector equation degenerates to:

$$\rho\frac{\mathrm{d}\boldsymbol{v}}{\mathrm{d}t} = \nabla\cdot\boldsymbol{\sigma} + \rho\,\boldsymbol{f} \quad \Rightarrow \quad \frac{\mathrm{d}p}{\mathrm{d}r} = -\rho\,(r)\,\frac{\mathrm{d}U^f}{\mathrm{d}r}. \tag{2.25}$$

After combining and integrating we obtain:

$$p\,(r) = p_0 - \int_{\bar{r}=0}^{\bar{r}=r}\frac{\rho\,(\bar{r})\,m\,(\bar{r})}{\bar{r}^2}\,\mathrm{d}\bar{r}. \tag{2.26}$$

In fact, it is this equation that is depicted in Fig. 2.4, which, of course, agrees with the pressure data presented in Table II of [17]. Clearly, a radially dependent mass density is difficult to incorporate in the fluid model for the flattening presented above. However, in view of the extreme underestimate of the center pressure in the simple fluid model as evident in Fig. 2.4 (right), it is absolutely essential to take it into account. In order to simulate the onion layered structure of the Earth we will discuss at the end of the paper the potential of combining the fluid and the solid model for predicting the flattening.

3 A linear-elastic solid model for the flattening

The solution presented in this section follows a procedure from a paper by Hiramatsu and Oka [26]. It can also found in great detail in [9], Section (9.6). We start from the stationary local balance of momentum in the ***co-moving non-inertial frame*** in spherical coordinates ignoring all explicit azimuthal dependences on φ:

$$\frac{\partial\sigma_{rr}}{\partial r}+\frac{1}{r}\frac{\partial\sigma_{r\vartheta}}{\partial\vartheta}+\frac{1}{r}(2\sigma_{rr}-\sigma_{\vartheta\vartheta}-\sigma_{\varphi\varphi}+\sigma_{r\vartheta}\cot\vartheta)=\rho_0(\frac{Gm_0}{R^3}-\omega_0^2)r+\rho_0\omega_0^2 r\cos^2\vartheta,$$

$$\begin{aligned}\frac{\partial\sigma_{r\vartheta}}{\partial r}+\frac{1}{r}\frac{\partial\sigma_{\vartheta\vartheta}}{\partial\vartheta}+\frac{1}{r}\left[3\sigma_{r\vartheta}+(\sigma_{\vartheta\vartheta}-\sigma_{\varphi\varphi})\ \cot\vartheta\right] &= -\rho_0\omega_0^2 r\sin\vartheta\cos\vartheta, \qquad (3.1)\\ \frac{\partial\sigma_{r\varphi}}{\partial r}+\frac{1}{r}\frac{\partial\sigma_{\vartheta\varphi}}{\partial\vartheta}+\frac{1}{r}\left(3\sigma_{r\varphi}+2\sigma_{\vartheta\varphi}\cot\vartheta\right) &= 0.\end{aligned}$$

For convenience we omit the dashes when denoting the position $\boldsymbol{x}'=r\boldsymbol{e}_r'$ and derivatives in the formulae, *i.e.*, we write (r,ϑ,φ) and not (r',ϑ',φ'). Likewise we write σ_{ij}, u_i and not σ_{ij}', u_i'. The expressions on the right hand side follow from the gravitational and centrifugal potentials shown in Eqns. (2.5) and (2.7). A homogeneous mass density, ρ_0, was assumed throughout. This is in agreement with the conventions of linear elasticity where the forces are applied to the ***undeformed*** system, which in the present case is a sphere of radius R and total mass $m=\frac{4\pi}{3}\rho_0 R^3$. We now complement these equations by Hooke's law into which linear kinematic conditions for the displacements $\boldsymbol{u}$ are inserted:

$$\sigma_{rr}=\lambda\Delta+2\mu\frac{\partial u_r}{\partial r},\quad \sigma_{\vartheta\vartheta}=\lambda\Delta+\frac{2\mu}{r}\left(\frac{\partial u_\vartheta}{\partial\vartheta}+u_r\right),$$

$$\sigma_{\varphi\varphi}=\lambda\Delta+\frac{2\mu}{r}\left(u_r+u_\vartheta\cot\vartheta\right),\sigma_{r\vartheta}=\mu\left[\frac{\partial u_\vartheta}{\partial r}-\frac{1}{r}\left(u_\vartheta-\frac{\partial u_r}{\partial\vartheta}\right)\right], \qquad (3.2)$$

$$\sigma_{\vartheta\varphi}=\frac{\mu}{r}\left(\frac{\partial u_\varphi}{\partial\vartheta}-u_\varphi\cot\vartheta\right),\sigma_{r\varphi}=\mu\left(\frac{\partial u_\varphi}{\partial r}-\frac{1}{r}u_\varphi\right)$$

with the following abbreviation:

$$\Delta=\frac{1}{r^2\sin\vartheta}\left[\frac{\partial}{\partial r}(r^2u_r\sin\ \vartheta)+\frac{\partial}{\partial\vartheta}(ru_\vartheta\sin\vartheta)\right]. \qquad (3.3)$$

λ and μ denote Lamé's constants. It is now a matter of differentiation and algebra to show that Eqns. $(3.1)_{1,2}$ can be rewritten as follows:

$$\begin{aligned}(\lambda+2\mu)\frac{\partial\Delta}{\partial r}-\frac{2\mu}{r}\frac{\partial\Omega}{\partial\vartheta}-\frac{2\mu}{r}\Omega\cot\vartheta &= \rho_0(\frac{Gm_0}{R^3}-\omega_0^2)r+\rho_0\omega_0^2 r\cos^2\vartheta, \qquad (3.4)\\ (\lambda+2\mu)\frac{1}{r}\frac{\partial\Delta}{\partial\vartheta}+2\mu\frac{\partial\Omega}{\partial r}+2\mu\frac{\Omega}{r} &= -\rho_0\omega_0^2 r\sin\vartheta\cos\vartheta\end{aligned}$$

with yet another abbreviation:

$$2\Omega = \frac{\partial u_\vartheta}{\partial r} + \frac{u_\vartheta}{\partial r} - \frac{1}{r}\frac{\partial u_r}{\partial \vartheta}. \tag{3.5}$$

We will return to Eqn. $(3.1)_3$ later. It will serve to determine and is ignored for the time being. Cross-differentiation of Eqns. (3.4) and mutual insertion leads to the decoupling of Δ and Ω:

$$\begin{aligned}
&\frac{\partial^2\Delta}{\partial r^2} + \frac{2}{r}\frac{\partial\Delta}{\partial r} + \frac{1}{r^2}\frac{\partial^2\Delta}{\partial\vartheta^2} + \frac{\cot\vartheta}{r^2}\frac{\partial\Delta}{\partial\vartheta} = \frac{\rho_0(\frac{3Gm_0}{R^3} - 2\omega_0^2)}{\lambda+2\mu}, \\
&\frac{\partial^2\Omega}{\partial r^2} + \frac{2}{r}\frac{\partial\Omega}{\partial r} + \frac{1}{r^2}\frac{\partial^2\Omega}{\partial\vartheta^2} + \frac{\cot\,\vartheta}{r^2}\frac{\partial\Omega}{\partial\vartheta} - \frac{\Omega}{(r\sin\vartheta)^2} = 0.
\end{aligned} \tag{3.6}$$

These are equations of the Legendre-type and we may write their general solution in terms of Legendre series:

$$\begin{aligned}
\Delta &= \frac{\rho_0(\frac{3Gm_0}{R^3} - 2\omega_0^2)}{6(\lambda+2\mu)} + \sum_{n=0}^{\infty}\left(A_n r^n - \frac{B_n}{r^{n+1}}\right)P_n, \\
\Omega &= \sum_{n=0}^{\infty}\left(a_n r^n - \frac{b_n}{r^{n+1}}\right)\frac{\mathrm{d}P_n}{\mathrm{d}\vartheta}.
\end{aligned} \tag{3.7}$$

$P_n = P_n(\cos\vartheta)$ denotes the Legendre polynomial of the n-th degree. Note that in the formula for Δ the particular solution has been taken into account so that the inhomogeneity of the corresponding differential equation is covered. Moreover, the coefficients used to express Ω are related to those of Δ since Eqns. (3.4) have to be observed. This leads to:

$$2\Omega = -\frac{\lambda+2\mu}{\mu}\sum_{n=0}^{\infty}\left(\frac{A_n}{n+1}r^n + \frac{B_n}{n}\frac{1}{r^{n+1}}\right)\frac{\mathrm{d}P_n}{\mathrm{d}\vartheta} + \frac{\rho_0\omega_0^2}{9\mu}r^2\frac{\mathrm{d}P_2}{\mathrm{d}\vartheta}. \tag{3.8}$$

These solutions help to find expressions for the two unknown displacements u_r and u_ϑ. To this end we use the definitions shown in Eqns. (3.3) and (3.5) to obtain:

$$\begin{aligned}
&\frac{\partial^2 u_\vartheta}{\partial r^2} + \frac{1}{r^2}\frac{\partial^2 u_\vartheta}{\partial\vartheta^2} + \frac{4}{r}\frac{\partial u_\vartheta}{\partial r} + \frac{\cot\vartheta}{r^2}\frac{\partial u_\vartheta}{\partial\vartheta} + \frac{1}{r^2}\left(2 - \frac{1}{\sin^2\vartheta}\right)u_\vartheta \\
&\qquad = \frac{\partial(2\Omega)}{\partial r} + \frac{1}{r}\frac{\partial\Delta}{\partial\vartheta} + \frac{3}{r}(2\Omega).
\end{aligned} \tag{3.9}$$

By observing Eqns. (3.7) and (3.8) we see that the solution to this differential equation is again of the Legendre-type:

$$\begin{aligned}
u_\vartheta = \sum_{n=0}^{\infty}\Bigg[&-\frac{(n+3)\lambda+(n+5)\mu}{(n+1)(2n+3)2\mu}A_n r^{n+1} \\
&-\frac{(n-2)\lambda+(n-4)\mu}{n(2n-1)2\mu}\frac{B_n}{r^n} + C_n r^{n-1} - \frac{D_n}{r^{n+2}}\Bigg]\frac{\mathrm{d}P_n}{\mathrm{d}\vartheta} + \frac{5\rho_0\omega_0^2}{126\mu}r^3\frac{\mathrm{d}P_2}{\mathrm{d}\vartheta}.
\end{aligned} \tag{3.10}$$

Now that we have found u_ϑ we can obtain the radial displacement by integration from Eqns. (3.3) and (3.5). If we suppress rigid body translation the final result reads:

$$u_r = \sum_{n=0}^{\infty} \left[-\frac{n\lambda + (n-2)\mu}{(2n+3)2\mu} A_n r^{n+1} + \frac{(n+1)\lambda + (n+3)\mu}{(2n-1)2\mu} \frac{B_n}{r^n} + nC_n r^{n-1} \right. \\ \left. + (n+1)\frac{D_n}{r^{n+2}} \right] P_n + \frac{\rho_0 \left(\frac{3Gm_0}{R^3} - 2\omega_0^2 \right)}{30\,(\lambda + 2\mu)} r^3 + \frac{\rho_0 \omega_0^2}{21\mu} r^3 P_2. \tag{3.11}$$

Finally we obtain u_φ by combining Eqns. $(3.1)_3$ and $(3.2)_{5,6}$:

$$u_\varphi = \sum_{n=1}^{\infty} \left(E_n r^n + \frac{F_n}{r^{n+1}} \right) \frac{\mathrm{d}P_n}{\mathrm{d}\vartheta}. \tag{3.12}$$

Before we turn to expressions for the stresses we try to simplify the series as much as possible by evaluating the following boundary conditions:

$$u_{r \text{ and } \vartheta}|_{r=0} < \infty \quad \Rightarrow \quad B_n = 0\ ,\ n = 1,\ 2,\ \cdots, D_n = 0\ ,\ n = 0,\ 1,\ \cdots, \\ u_r|_{r=0} = 0 \Rightarrow\ B_0 = 0, C_1 = 0, u_\varphi|_{r=0} < \infty \quad \Rightarrow \quad F_n = 0\ ,\ n = 1,\ 2,\ \cdots. \tag{3.13}$$

Note that C_0 and F_0 are irrelevant because of the prefactor n and $\mathrm{d}P_0/\mathrm{d}\vartheta = 0$, respectively. Thus according to Eqns. (3.2) the stresses relevant for traction boundary conditions at the outer surface read:

$$\sigma_{rr} = \sum_{n=0}^{\infty} \left[-\frac{(n^2 - n - 3)\lambda + (n+1)(n-2)\mu}{2n+3} A_n r^n + n(n-1)2\mu C_n r^{n-2} \right] P_n \\ + \frac{5\lambda + 6\mu}{10} \frac{\rho_0 \frac{Gm_0}{R^3}}{\lambda + 2\mu} r^2 - \frac{5\lambda + 6\mu}{15} + \frac{\rho_0 \omega_0^2}{\lambda + 2\mu} r^2 + \frac{2}{7} \rho_0 \omega_0^2 r^2 P_2, \tag{3.14}$$

$$\sigma_{r\vartheta} = \sum_{n=1}^{\infty} \left[-\frac{n(n+2)\lambda + (n^2 + 2n - 1)\mu}{(n+1)(2n+3)} A_n r^n + 2\mu(n-1) C_n r^{n-2} \right] \frac{\mathrm{d}P_n}{\mathrm{d}\vartheta} \\ + \frac{8}{63} \rho_0 \omega_0^2 r^2 \frac{\mathrm{d}P_2}{\mathrm{d}\vartheta},$$

$$\sigma_{r\varphi} = \mu \sum_{n=1}^{\infty} (n-1) E_n r^{n-1} \frac{\mathrm{d}P_n}{\mathrm{d}\vartheta}.$$

The traction vector at the outer surface $r = R$ vanishes and:

$$\sigma_{r\varphi}|_{r=R} = 0 \Rightarrow E_n = 0, \quad n = 2, 3, \cdots, \tag{3.15}$$

because of the linear independence of the polynomial expressions $\mathrm{d}P_n/\mathrm{d}\vartheta$. We conclude that:

$$\sigma_{r\varphi} \equiv 0, \quad u_\varphi \equiv 0. \tag{3.16}$$

Moreover:

$$\sigma_{r\vartheta}|_{r=R} = 0 \Rightarrow$$

$$n \neq 2: \quad -\frac{n(n+2)\lambda + (n^2+2n-1)\mu}{(n+1)(2n+3)} R^n A_n + 2\mu(n-1)R^{n-2}C_n = 0, \tag{3.17}$$

$$n = 2: \quad -\frac{8\lambda+7\mu}{21} R^2 A_2 + 2\mu\, C_2 + \frac{8}{63}\rho_0\omega_0^2 R^2 = 0.$$

And finally:

$$\sigma_{rr}|_{r=R} = 0 \Rightarrow$$

$$n = 0: \quad \frac{5\lambda+6\mu}{10}\frac{\rho_0\frac{Gm_0}{R^3}}{\lambda+2\mu}R^2 - \frac{5\lambda+6\mu}{15}\frac{\rho_0\omega_0^2}{\lambda+2\mu}R^2 + \frac{3\lambda+2\mu}{3}A_0 = 0,$$

$$n = 1: \quad \frac{3\lambda+2\mu}{7}RA_1 = 0 \quad \Rightarrow \quad A_1 = 0, \tag{3.18}$$

$$n = 2: \quad \frac{2}{7}\rho_0\omega_0^2 R^2 + \frac{\lambda}{7}A_2 R^2 + 4\mu\, C_2 = 0,$$

$$n > 2: \quad -\frac{(n^2-n-3)\lambda + (n+1)\,(n-2)\mu}{(2n+3)} R^n A_n$$
$$+2\mu\, n(n-1)R^{n-2}C_n = 0.$$

We are now in a position to determine all remaining coefficients:

$$A_0 = -\frac{3}{10}\frac{5\lambda+6\mu}{3\lambda+2\mu}\frac{\rho_0\frac{Gm_0}{R^3}}{\lambda+2\mu}R^2 + \frac{1}{5}\frac{5\lambda+6\mu}{3\lambda+2\mu}\frac{\rho_0\omega_0^2}{\lambda+2\mu}R^2,$$

$$A_1 = 0, A_2 = -\frac{2}{3}\frac{\rho_0\omega_0^2}{19\lambda+14\mu}, A_n = 0\ , \quad n = 3,\ 4,\ \cdots, \tag{3.19}$$

$$C_2 = -\frac{4\lambda+3\mu}{19\lambda+14\mu}\frac{\rho_0\omega_0^2}{3\mu}R^2, C_n = 0\ , \quad n = 3,\ 4,\ \cdots.$$

The stresses are now explicit:

$$\sigma_{rr} = -\left[\frac{1}{10}\frac{3-\nu}{1-\nu}\left(\frac{g}{a_c} - \frac{2}{3}\right) + \frac{2}{3}\frac{3+2\nu}{7+5\nu}P_2\right](1 - \frac{r^2}{R^2})\rho_0\omega_0^2 R^2,$$

$$\sigma_{\vartheta\vartheta} = -\left(\frac{1}{10}\frac{3-\nu}{1-\nu}\left(\frac{g}{a_c} - \frac{2}{3}\right)\left(1 - \frac{1+3\nu}{3-\nu}\frac{r^2}{R^2}\right)\right. \tag{3.20}$$
$$\left. + \frac{3+2\nu}{3(7+5\nu)}\left[2P_2\left(1 - \frac{1}{3+2\nu}\frac{r^2}{R^2}\right) + \frac{\mathrm{d}^2P_2}{\mathrm{d}\vartheta^2}\left(1 - \frac{2+\nu}{3+2\nu}\frac{r^2}{R^2}\right)\right]\right)\rho_0\omega_0^2 R^2,$$

$$\sigma_{\varphi\varphi} = -\left(\frac{1}{10}\frac{3-\nu}{1-\nu}\left(\frac{g}{a_c} - \frac{2}{3}\right)\left(1 - \frac{1+3\nu}{3-\nu}\frac{r^2}{R^2}\right)\right.$$
$$\left. + \tfrac{1}{3}\left[\left(\frac{2(1+\nu)}{4+5\nu}P_2 + \frac{2+\nu}{7+5\nu}\right)\frac{r^2}{R^2} - \frac{3+2\nu}{7+5\nu}\right]\right)\rho_0\omega_0^2 R^2$$

$$\sigma_{r\vartheta} = -\frac{3+2\nu}{3(7+5\nu)}\frac{\mathrm{d}P_2}{\mathrm{d}\vartheta}\left(1-\frac{r^2}{R^2}\right)\rho_0\omega_0^2R^2, \sigma_{r\varphi}=0, \sigma_{\vartheta\varphi}=0,$$

and so are the displacements:

$$u_r = -\frac{\rho_0\omega_0^2R^2}{E}\frac{(1+\nu)(1-2\nu)}{1-\nu}\left[\frac{1}{10}\left(\frac{g}{a_c}-\frac{2}{3}\right)\left(\frac{3-\nu}{1+\nu}-\frac{r^2}{R^2}\right)\right.$$
$$\left.+\frac{2(1-\nu)}{3(1-2\nu)}P_2\left(\frac{3+2\nu}{7+5\nu}-\frac{1+\nu}{7+5\nu}\frac{r^2}{R^2}\right)\right]r \qquad (3.21)$$

$$u_\vartheta = -\frac{\rho_0\omega_0^2R^2}{3E}(1+\nu)\frac{\mathrm{d}P_2}{\mathrm{d}\vartheta}\left(\frac{3+2\nu}{7+5\nu}-\frac{2+\nu}{7+5\nu}\frac{r^2}{R^2}\right)r, \quad u_\varphi = 0.$$

For further investigations it was advantageous to use Young's modulus, E, and Poisson's ratio, ν, instead of Lamé's constants:

$$\lambda = \frac{\nu}{(1-2\nu)(1+\nu)}E, \quad 2\mu = \frac{1}{1+\nu}E. \qquad (3.22)$$

Moreover, we have defined the gravitational and centrifugal accelerations at the outer (equatorial) surface $r = R$ by:

$$g = \frac{Gm}{R^2}, \quad a_\mathrm{c} = R\omega_0^2. \qquad (3.23)$$

As we shall see it is instructive to divide the stresses and displacements into purely gravitational and centrifugal parts:

$$\sigma_{ij} = \sigma_{ij}^{\mathrm{grav}} + \sigma_{ij}^{\mathrm{c}}, u_i = u_i^{\mathrm{grav}} + u_i^{\mathrm{c}}, i,j \in \{r,\vartheta,\varphi\}\,, \qquad (3.24)$$

where:

$$\sigma_{rr}^{\mathrm{grav}} = -\frac{3mg}{10A}\frac{3-\nu}{1-\nu}\left(1-\frac{r^2}{R^2}\right),$$
$$\sigma_{\vartheta\vartheta}^{\mathrm{grav}} \equiv \sigma_{\varphi\varphi}^{\mathrm{grav}} = -\frac{3mg}{10A}\frac{3-\nu}{1-\nu}\left(1-\frac{1+3\nu}{3-\nu}\frac{r^2}{R^2}\right),$$
$$\sigma_{r\vartheta}^{\mathrm{grav}} = 0\,, \quad \sigma_{r\varphi}^{\mathrm{grav}} = 0\,, \quad \sigma_{\vartheta\varphi}^{\mathrm{grav}} = 0, \qquad (3.25)$$
$$u_r^{\mathrm{grav}} = -\frac{mg}{10Ak}\frac{1+\nu}{1-\nu}\left(\frac{3-\nu}{1+\nu}-\frac{r^2}{R^2}\right)r, \quad u_\varphi^{\mathrm{grav}} = 0, \quad u_\varphi^{\mathrm{grav}} = 0,$$

and:

$$\begin{aligned}
\sigma^{\rm c}_{rr} &= \left(\tfrac{1}{10} - \frac{3+2\nu}{7+5\nu}P_2\right)\tfrac{2}{3}\left(1-\frac{r^2}{R^2}\right)\rho_0\omega_0^2R^2,\\
\sigma^{\rm c}_{\vartheta\vartheta} &= \left(\tfrac{1}{15}\frac{3-\nu}{1-\nu}\left(1-\frac{1+3\nu}{3-\nu}\frac{r^2}{R^2}\right) - \frac{3+3\nu}{3(7+5\nu)}\left[2P_2\left(1-\frac{1}{3+2\nu}\frac{r^2}{R^2}\right)\right.\right.\\
&\left.\left.+\frac{{\rm d}^2P_2}{{\rm d}\vartheta^2}\left(1-\frac{2+\nu}{3+2\nu}\frac{r^2}{R^2}\right)\right]\right)\rho_0\omega_0^2R^2,\\
\sigma^{\rm c}_{\varphi\varphi} &= \left(\tfrac{1}{15}\frac{3-\nu}{1-\nu}\left(1-\frac{1+3\nu}{3-\nu}\frac{r^2}{R^2}\right)\right.\\
&\left.-\tfrac{1}{3}\left[\left(\frac{2(1+\nu)}{7+5\nu}P_2+\frac{2+\nu}{7+5\nu}\right)\frac{r^2}{R^2}-\frac{3+2\nu}{7+5\nu}\right]\right)\rho_0\omega_0^2R^2,\\
\sigma^{\rm c}_{r\vartheta} &\equiv \sigma_{r\vartheta} = -\frac{3+2\nu}{3(7+5\nu)}\frac{{\rm d}P_2}{{\rm d}\vartheta}\left(1-\frac{r^2}{R^2}\right)\rho_0\omega_0^2R^2,\ \sigma^{\rm c}_{r\varphi}=0,\ \sigma^{\rm c}_{\vartheta\varphi}=0,
\end{aligned} \tag{3.26}$$

$$\begin{aligned}
u^{\rm c}_r &= \frac{\omega_0^2 m}{2\pi E}\frac{(1+\nu)(1-2\nu)}{1-\nu}\left[\tfrac{1}{10}\left(\frac{3-\nu}{1+\nu}-\frac{r^2}{R^2}\right)\right.\\
&\left.-\frac{1-\nu}{1-2\nu}P_2\left(\frac{3+2\nu}{7+5\nu}-\frac{1+\nu}{7+5\nu}\frac{r^2}{R^2}\right)\right]\frac{r}{R},
\end{aligned}$$

$$u^{\rm c}_\vartheta \equiv u_\vartheta = -\frac{\omega_0^2 m}{2\pi E}(1+\nu)\frac{{\rm d}P_2}{{\rm d}\vartheta}\left(\frac{3+2\nu}{7+5\nu}-\frac{2+\nu}{7+5\nu}\frac{r^2}{R^2}\right)\frac{r}{R},\ \ u^{\rm c}_\varphi = 0.$$

A denotes the surface area of the (spherical) celestial body. It is useful to introduce this quantity since the factor $\frac{gm}{A}$ can now be interpreted as the total "weight" of the celestial body distributed over its surface. This is nothing else but a pressure and it serves nicely as a very intuitive measure for normalizing the gravitational stresses and displacement. However, of course, we may also write $\frac{gm}{A} \equiv \frac{Gm^2}{4\pi R^4}$. As we shall see shortly this notation is more suitable if we wish to discuss the range of validity of the linear-elastic solution. Moreover, $k = \lambda + \frac{2}{3}\mu$, $2\mu = \frac{E}{1+\nu}$ denote the isotropic compressibility of a Hookean solid and its shear modulus, respectively. Gravity will compress the celestial body quite strongly and, therefore, it is most appropriate to use k in context with the gravitational part of the solution.

Fig. 3.1 presents a study of various aspects of the behavior of the gravitational part of the displacement. In a sphere gravity leads to purely radial contraction, *i.e.*, there is only a radial displacement, $u_r^{\rm grav}$. The first two pictures concentrate on the dimensionless form given by Eqn. $(3.25)_6$. The situation is depicted for three different values of Poisson's ratio: $\nu = 0$ (red), $\nu = 0.3$ (green), $\nu = 0.5$ (blue). If we normalize by E instead of k (second picture in Fig. 3.1), we can see very clearly that the radial contraction vanishes if $\nu = 0.5$, *i.e.*, if the body is incompressible, no matter how strong the gravitational force may be. This is an artifact inherent to the concept of incompressibility. It is

interesting to note that, depending on Poisson's ratio, the extremum of u_r^{grav} is not necessarily located at the surface of the celestial body. In fact, we find:

$$r^{\text{ext}} = \sqrt{\tfrac{1}{3}\frac{3-\nu}{1+\nu}}R. \tag{3.27}$$

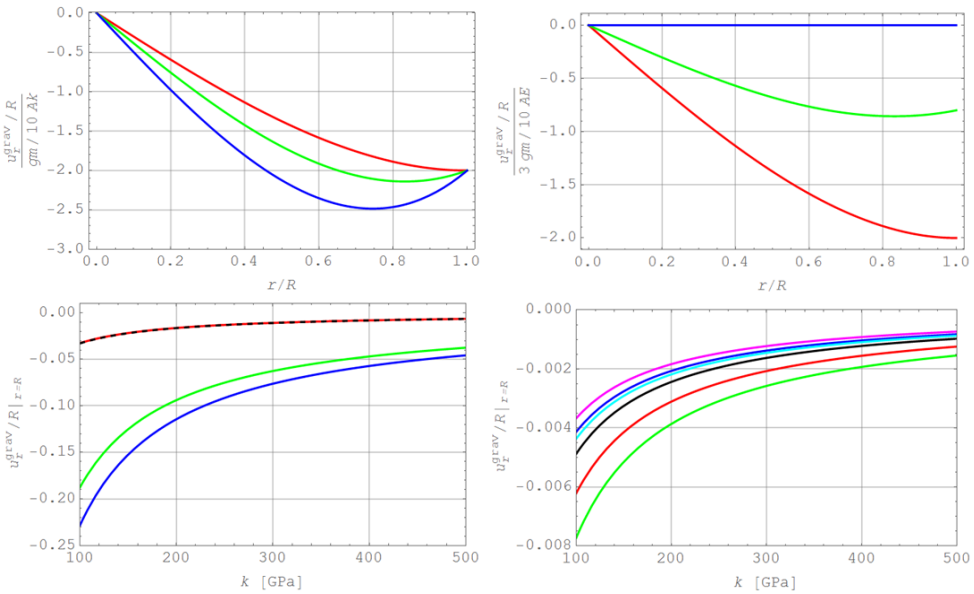

Fig. 3.1: Behavior of the radial gravitational displacement component (see text).

Note that at the surface of a celestial body we have:

$$u_r^{\text{grav}}/R|_{r=R} = -\frac{Gm^2}{20\pi R^4 k}. \tag{3.28}$$

The concept of linear elasticity is valid if the displacements, and in particular this expression, remain small. This may not necessarily be so for all telluric celestial bodies, which we would like to treat as solids, in particular by the model of a Hookean solid. We proceed to investigate this issue in the next two viewgraphs.

Fig. 3.1_3 is dedicated to the inner planets (Mercury in red, Venus in green, Earth in blue, and the dashed line for Mars). For the numerical evaluation we have used the mass data shown in Table 1. For the radius we use the values for $R \equiv a_1$. The latter choice is somewhat problematic: In order to meet the requirements of the linear theory of elasticity, we need to know the radius of the reference state, *i.e.*, the outer radius before loads have been applied, and not a radius that includes the effects of gravity and centrifugal acceleration. Thus our choice for R represents essentially the current radial situation. However, within the framework of linear elasticity the difference between the current and the reference radius should differ by a few percent, at most. Moreover, the proper choice of k is by no means obvious. Basically,

k is an average compressibility of the respective body. For that reason we have decided to depict Eqn. (3.28) for a physically reasonable range of k-values. Clearly, the linear theory of elasticity seems to be applicable only to Mercury and Mars (for which the values nearly coincide). Venus and Earth show normalized displacements of 5% and more, which are not acceptable. A non-linear approach is necessary to calculate the gravitational stresses and displacements in this case.

Fig. 3.1_4 focuses on various moons (Earth's Moon in red, Io in green, Europa in blue, Ganymede in black, Callisto in magenta, Titan in cyan). The necessary data is compiled in Table 2. We conclude that the linear-elastic solution applies.

The first two pictures in Fig. 3.2 show the non-vanishing dimensionless components of the centrifugal part of the displacement according to Eqn. $(3.26)_{7,8}$ for three different values of Poisson's ratio, namely $\nu = 0$ (red), $\nu = 0.3$ (green), and $\nu = 0.5$ (blue). u_r^{c} was evaluated at the equator, *i.e.*, $\vartheta = \pi/2$, and for the pole, *i.e.*, $\vartheta = 0$. This leads to positive and to negative values, respectively, which makes sense in view of the effect of the centrifugal acceleration on a deformable body (extension perpendicular to the axis of rotation accompanied by lateral contraction). u_ϑ^{c} was evaluated at the equator, *i.e.*, $\vartheta = \pi/4$, where it assumes its extremum. It is interesting to note that the extreme values are not necessarily located at the surface of the body and that the location depends on Poisson's ratio as follows:

$$\text{for} \quad u_r^{\mathrm{c}} \to r^{\mathrm{ext}} = \sqrt{\frac{1}{3}\frac{\frac{(1-2\nu)(3-\nu)}{1+\nu} - 10\frac{(1-\nu)(3+2\nu)}{(7+5\nu)}P_2}{1-2\nu-10\frac{(1-\nu)(1+\nu)}{7+5\nu}P_2}R}, \tag{3.29}$$

$$\text{for} \quad u_\vartheta^{\mathrm{c}} \to r^{\mathrm{ext}} = \sqrt{\frac{1}{3}\frac{3+2\nu}{2+\nu}R} \quad \text{(independently of } \vartheta\text{)}.$$

Table 2: Physical data for the Moon and some Jupiter and Saturn moons [27].

Moons	a_1 [m]	m [kg]
Moon	1.738E+06	7.34E+22
Io	1.82E+06	8.932E+22
Europa	1.56E+06	4.8E+22
Ganymede	2.63E+06	1.482E+23
Callisto	2.41E+06	1.08E+23
Titan	2.576E+06	1.3452E+23

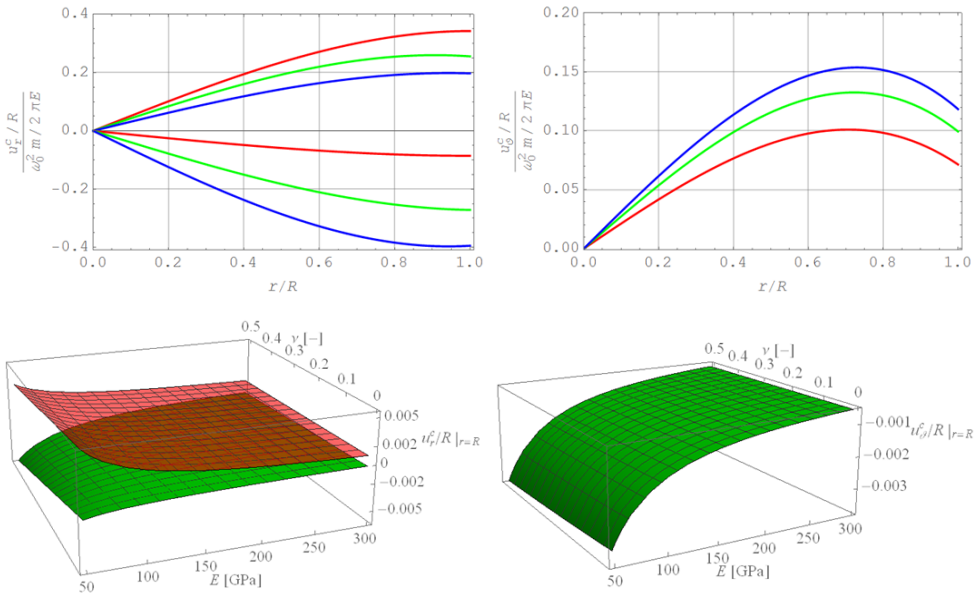

Fig. 3.2: Behavior of the centrifugal displacement components (see text).

We now concentrate specifically on the Earth and find for the centrifugal displacement components on its surface:

$$u_r^{\mathrm{c}}/R|_{r=R} = \frac{\omega_{0,\mathrm{E}}^2 m_{\mathrm{E}}}{2\pi E}\left[\tfrac{1}{5}(1-2\nu) - \frac{(1+\nu)(2+\nu)}{7+5\nu}P_2\right], \tag{3.30}$$

$$u_r^{\mathrm{c}}/R|_{r=R} = \frac{\omega_{0,\mathrm{E}}^2 m_{\mathrm{E}}}{4\pi E}\left[\tfrac{1}{5}(1-2\nu) - \frac{(1+\nu)(2+\nu)}{7+5\nu}P_2\right].$$

The third and fourth picture in Fig. 3.2 illustrate these relationships when evaluated in the equatorial plane, $u_r^{\mathrm{c}}/R|_{\vartheta=\pi/2}$, (positive values due to centrifugal acceleration), in the polar direction, $u_r^{\mathrm{c}}/R|_{\vartheta=0}$, (negative values due to lateral contraction, *i.e.*, the Poisson effect), and at 45°, $u_\vartheta^{\mathrm{c}}/R|_{\vartheta=\pi/4}$, using Earth data from Table 1 (with $R = a_1$) for physically reasonable ranges of Young's modulus and Poisson's ratios. Obviously, all values stay below the 1% threshold and, hence, the message is that linear elasticity may be used to describe the centrifugal displacements and stresses even in the case of the Earth. We now compute the flattening in general as follows:

$$a = R + u_r(r=R,\ \vartheta=\pi/2),\quad c = R + u_r(r=R,\ \vartheta=0) \tag{3.31}$$

$$\Rightarrow \quad f \equiv \frac{a-c}{a} \approx \frac{\rho_0 R^2\omega_0^2}{E}\frac{(1+\nu)\ (2+\nu)}{7+5\nu} \equiv \frac{\rho_0 R^2\omega_0^2}{\mu}\frac{1+\nu/2}{7+5\nu},$$

if we neglect higher order terms in u_r as we should within the framework of a linear theory.

This, indeed, is the result originally presented by Thomson and Tait in [4], pg. 432. However, in comparison with Eqn. (2.13) from the fluid model this relation has a serious drawback: For a given telluric body it is not evident which effective elastic constants, *i.e.*, Young's modulus and Poisson's ratio, to use. However, if we believe that this simple Hookean model applies to telluric planets we may use this result to determine an effective shear modulus or modulus of rigidity, $\mu \equiv G$, if we use the experimentally observed data for the flattening. The factor $\frac{1+\nu/2}{7+5\nu}$ is nearly constant for all possible values of ν. *i.e.*, ca. 1/7:

$$\mu = \frac{3m\omega_0^2}{28\pi Rf}. \tag{3.32}$$

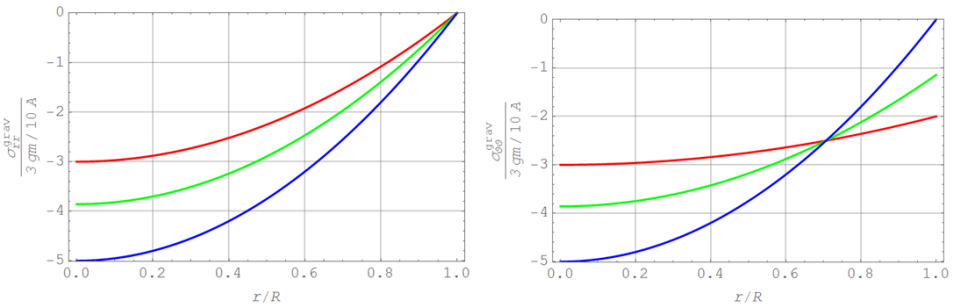

Fig. 3.3: Behavior of the gravitational stress components (see text).

If we evaluate this relation using Earth's data we obtain a value of 50 GPa, which is smaller than the value for iron or steel (roughly 70 GPa), which is often quoted in context with planet Earth.

We now turn to the stresses and begin by examining the purely gravitational part shown in Eqns. (3.25). As it should, these relations are of a purely radial nature: There are no shear stresses, all normal stresses depend only on the radius r, and the two angular stresses are equal. Fig. 3.3 illustrates their dependence on r for three different choices of Poisson's ratio, $\nu = 0$ (red), $\nu = 0.3$ (green), and $\nu = 0.5$ (blue). The maximum compression is at the body's center. Interesting to note is the cross-over point of the angular stresses. It is independent on Poisson's ratio and located at $r/R = \sqrt{\frac{1}{2}}$.

It should be pointed out that the linear-elastic solution for the gravitational part is dominant in comparison with the stresses due to centrifugal accelerations. Fig. 3.4 illustrates the situation by showing the behavior of all ***combined stresses*** according to Eqn. (3.20) as a function of radial position for various values of Poisson's ratio. In fact, the plots for the normal stresses were generated for the equatorial plane, *i.e.*, by choosing $\vartheta = \pi/2$, and the one for the shear stress at $\vartheta = \pi/4$ in order to show the maximum values. For the numerical evaluation we have chosen the observed mean radius of the Earth, *i.e.*, $R_{\rm E} = 6.371 \cdot 10^6$m, $\omega_{0,\rm E} = 2\pi/86,164$ s, and $m_{\rm E} = 5.97 \cdot 10^{24}$kg [7]. Thus we have $g = 9.81\frac{\rm m}{\rm s^2}$, $a_{\rm c} = 0.034\frac{\rm m}{\rm s^2}$, and $\frac{g}{a_{\rm c}} = 298.7$. These numbers already indicate the dominance of gravitation. In fact, in the case of the

normal stresses it turns out that the gravitational parts in Eqn. (3.20) are so strong that they conceal the dependence on the polar angle almost completely. All normal stresses are highly compressive. Note the striking similarity to the plots shown in Fig. 3.3 and the very slight difference between the two angular stresses. Both emphasizes our point that gravitation is dominant. Moreover, the shear stress is hardly dependent on Poisson's ratio.

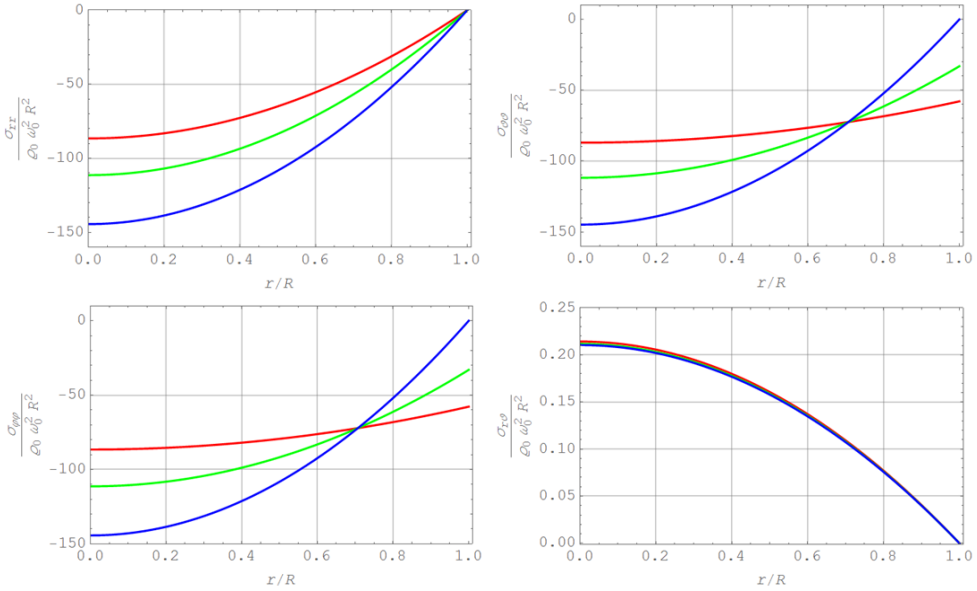

Fig. 3.4: Behavior of the combined stress components (see text).

There is another *caveat* we have to keep in mind, specifically in context with the Earth. During our discussion of the displacements due to gravitation we found that the linear-elastic solution is not really valid for planet Earth: The predicted displacements were simply too large (see Fig. 3.1_3). To be specific, the radius we chose for our numerical evaluation of the stresses in Fig. 3.4 is the ***observed*** mean radius, *i.e.*, the radius after gravitation and centrifugal accelerations are "switched on." The symbol R in our linear-elastic calculations, however, is the radius of the ***unloaded*** configuration. In other words, it is much larger than the chosen $R_{\mathrm{E}} = 6.371 \cdot 10^6$m. Thus, the predicted magnitude of the combined normal stresses is doubtful, too: Our numerical value ***underestimates*** distances in the reference configuration and the ratio $\frac{g}{a_c} \equiv \frac{G m_{\mathrm{E}}}{R_{\mathrm{E}}^3 \omega_{0,\mathrm{E}}^2}$ will become smaller. Most likely it will keep its dominance in the stress expressions, but the details are left to a non-linear analysis and future research.

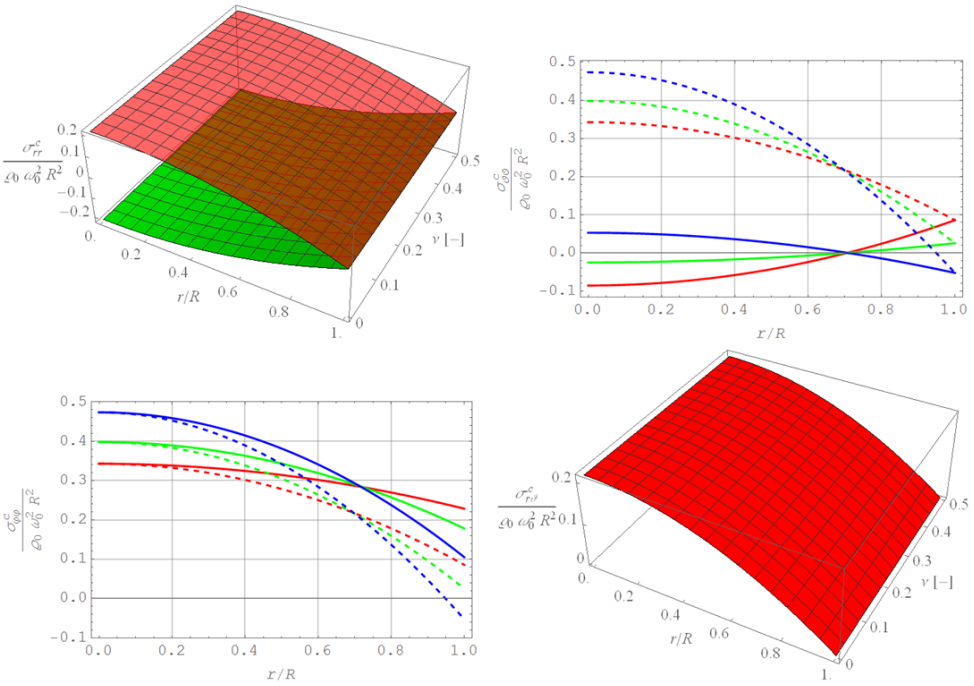

Fig. 3.5: Behavior of the centrifugal stress components (see text).

There is no problem with a numerical evaluation of the shear stress, though, since it is purely due to centrifugal acceleration. For conversion of the numbers shown on all plots in Fig. 3.4 into absolute stress values we may use $\rho_{0,\mathrm{E}} R_{\mathrm{E}}^0 \approx$ 119 GPa in case of the Earth. Thus the shear stresses within this simplistic model are very small. For example, they amount to ca. 0.1 MPa one km below they Earth's surface. This is in favor of the low shear stress hypothesis as outlined, *e.g.*, on pg. 543 of [28]. However, we have to keep in mind that this is a very simplistic Earth model, although an exact and quantitative one.

Fig. 3.5 illustrates the behavior of all stress components due to centrifugal acceleration as given by Eqn. $(3.26)_{1-6}$. The radial as well as the shear stress show hardly any dependence on Poisson's ratio. Their behavior is depicted in Figs. $3.5_{1,4}$. σ^{c}_{rr} was evaluated along the equator at $\vartheta = \pi/2$ and along the radius leading to the pole, *i.e.*, $\vartheta = 0$, giving positive and negative values, respectively, as intuitively expected. $\sigma^{\mathrm{c}}_{r\vartheta}$ was drawn for $\vartheta = \pi/4$ at the location of maximum values. The angular normal stresses show a distinct dependence on ν. They were evaluated for three different choices of Poisson's ratio, $\nu = 0$ (red), $\nu = 0.3$ (green), and $\nu = 0.5$ (blue) at $\vartheta = \pi/2$ (solid lines) and $\vartheta = 0$ (dashed lines).

We now turn to a study of the mechanical pressure. If we restrict ourselves to gravitation we may write:

$$p^{\mathrm{grav}} = -\tfrac{1}{3}(\sigma^{\mathrm{grav}}_{rr} + \sigma^{\mathrm{grav}}_{\vartheta\vartheta} + \sigma^{\mathrm{grav}}_{\varphi\varphi}) = \frac{gm}{10A}\frac{3-\nu}{1-\nu}\left(3 - \frac{5(1+\nu)}{3-\nu}\frac{r^2}{R^2}\right). \qquad (3.33)$$

Note that because of $\frac{3gm}{A} \equiv \frac{\rho_0 Gm}{R}$ this reduces to the pressure distribution for the gravitationally stressed, incompressible liquid sphere shown in Eqn. (2.22), if we only use the incompressibility condition $\nu = 0.5$ for a Hookean solid. We might have suspected this, even if an incompressible Hookean solid should not be referred to as an incompressible fluid.

Fig. 3.6 depicts the total mechanical pressure, which was calculated from:

$$p = -\tfrac{1}{3}(\sigma_{rr} + \sigma_{\vartheta\vartheta} + \sigma_{\varphi\varphi}), \tag{3.34}$$

i.e., the combined action of gravitation and centrifugal acceleration. The equation was evaluated for $\vartheta = \pi/2$ using Eqn. (3.20) and Earth data. The same color code as before applies. However, as expected from our previous discussion, gravitation is dominant. In other words the plots look essentially the same for other values of ϑ. Note the agreement with Fig. 2.4 (right) for the case $\nu = 0.5$. The curious cross-over point is visible again and the predicted pressure are well below the ones predicted by the PREM model. Clearly the calculation of the pressure according to Eqns. (3.33/34) is formal and does not satisfy the boundary condition $p(r/R) = 0$ unless the incompressibility condition $\nu = 0.5$ is satisfied.

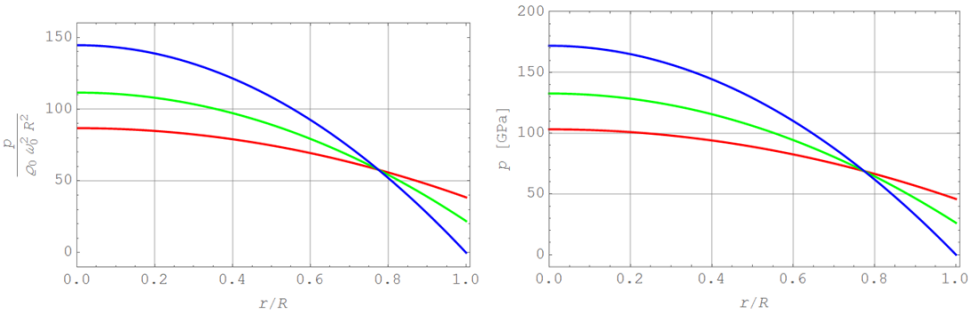

Fig. 3.6: Mechanical pressure as a function of the dimensionless radius, r/R, (see text).

4 Investigations based on global balances

The following arguments are rather independent of the constitutive model used for the celestial body, *i.e.*, they apply to the fluid as well as to the Hookean model. We start by considering a spherical, non-rotating (w.r.t. the inertial frame of reference) Earth of radius R, that transforms gradually and dynamically into the final equilibrium state of a spheroid of dimensions a and c rotating at a constant angular speed, ω_0. In the case of the energy balance it will be opportune to perform this transformations in two steps: First, the Initially non-rotating sphere, (I), is accelerated and becomes a spherical body rotating at ω_0. Second, this virtual, Intermediate state (I*) is allowed to relax into the Final spheroidal shape, (F). However, in the case of the integral or global ***mass balance*** this distinction is unnecessary. We easily integrate between the initial and the final state w.r.t. time and obtain:

$$\frac{\mathrm{d}}{\mathrm{d}t}\int_{V(t)} \rho \, \mathrm{d}V = 0 \quad \Rightarrow \quad \rho_0 \int_{V(t_\mathrm{F})} \mathrm{d}V' = \rho_0 \int_{V(t_\mathrm{I})} \mathrm{d}V. \tag{4.1}$$

Here we have assumed that the fluid is incompressible. Moreover, the volume will be determined in co-moving Cartesian coordinates. In the case of a sphere the integration is of high school level. For the spheroid we use (from Eqn. (2.18)):

$$\mathrm{d}V' = a^2 c \; \xi_1^2 \sin\xi_3 \mathrm{d}\xi_1 \mathrm{d}\xi_2 \mathrm{d}\xi_3, \tag{4.2}$$

and find:

$$\frac{R}{a} = f^{1/3}. \tag{4.3}$$

This relation will become very useful later in context with the energy balance.

We now turn to the global **balance of momentum** for an inertial system located at the center of gravity of Earth:

$$\frac{\mathrm{d}}{\mathrm{d}t}\int_{V(t)} \rho \, \boldsymbol{v} \, \mathrm{d}V = \oint_{\partial V(t)} \boldsymbol{n}\cdot\boldsymbol{\sigma} \, \mathrm{d}A - \int_{V(t)} \rho \, \nabla U^f(\boldsymbol{x}) \, \mathrm{d}V. \tag{4.4}$$

Note that in contrast to Eqn. (2.6) the gravitational potential being a scalar function is expressed and differentiated w.r.t. the position vector $\boldsymbol{x}$ expressed in the inertial system. Of course, due to $\boldsymbol{b} = \boldsymbol{0}$ in the Euclidean transformation $(2.1)_1$ we have $\boldsymbol{x} = \boldsymbol{x}'$. The left hand side is easy to integrate between the initial and the final state:

$$\int_{t_\mathrm{I}}^{t_\mathrm{F}} \frac{\mathrm{d}}{\mathrm{d}t}\int_{V(t)} \rho \, \boldsymbol{v} \, \mathrm{d}V\mathrm{d}t = \int_{V(t_\mathrm{F})} \rho \, \boldsymbol{v} \, \mathrm{d}V - \boldsymbol{0}, \tag{4.5}$$

because the Earth does not move initially. However, in the end Earth particles move according to $(2.1)_2$, *i.e.*:

$$\boldsymbol{v} = \boldsymbol{\omega} \times \boldsymbol{x}'. \tag{4.6}$$

Thus, by using $\boldsymbol{\omega} = \omega_0\, \boldsymbol{e}'_3$, $\boldsymbol{x}' = x'_i \boldsymbol{e}'_i$, and $\mathrm{d}V = \mathrm{d}V'$ we find:

$$\int_{V(t_\mathrm{F})} \rho\, \boldsymbol{v}\, \mathrm{d}V = \omega_0 \left(-\boldsymbol{e}'_1 \int_{V'(t_\mathrm{F})} \rho\, x'_2\, \mathrm{d}V' + \boldsymbol{e}'_2 \int_{V'(t_\mathrm{F})} \rho\, x'_1\, \mathrm{d}V' \right) \equiv \boldsymbol{0}, \tag{4.7}$$

because the center of the non-inertial system coincides with the center of gravity, just like the center of the inertial system.

Note that we did not have to make use of the constancy of the mass density. We conclude that the translational momentum of the Earth in co-moving frames vanishes, as expected all along. Consequently, the right hand side of the time-integrated version of Eqn. (4.4) must vanish, too:

$$\int_{t_\mathrm{I}}^{t_\mathrm{F}} \oint_{\partial V(t)} \boldsymbol{n} \cdot \boldsymbol{\sigma}\, \mathrm{d}A\, \mathrm{d}t - \int_{t_\mathrm{I}}^{t_\mathrm{F}} \int_{V(t)} \rho\, \nabla U^f(\boldsymbol{x})\, \mathrm{d}V \mathrm{d}t \equiv \boldsymbol{0}. \tag{4.8}$$

In fact, the second integrand representing the contribution of the gravitational forces to the impulse (*Kraftstoss*) vanishes under certain prerequisites. First, we assume incompressibility, rewrite the expression by using Gauss' theorem, and add and subtract a term representing the centrifugal forces, respectively:

$$\begin{aligned} &\rho_0 \int_{V(t)} \nabla U^f(\boldsymbol{x})\, \mathrm{d}V \\ &= \rho_0 \left(\oint_{\partial V(t)} \boldsymbol{n} \left[U^f(\boldsymbol{x}) + U^\omega(\boldsymbol{x}) \right] \mathrm{d}A - \int_{V'(t)} \nabla' U^\omega(\boldsymbol{x}')\, \mathrm{d}V' \right). \end{aligned} \tag{4.9}$$

Note that because of (2.5) and $\boldsymbol{x} = \boldsymbol{x}'$ we have $U^\omega(\boldsymbol{x}) = U^\omega(\boldsymbol{x}')$, which explains the second part in the surface integral which originally stemmed from the added term. If we now assume that the process during which the angular velocity increases is slow, we may regard the system surface $\partial V(t)$ to be an equipotential surface at all times t and write:

$$\begin{aligned} &\oint_{\partial V(t)} \boldsymbol{n}\, \left[U^f(\boldsymbol{x}) + U^\omega(\boldsymbol{x}) \right] \mathrm{d}A \\ &= \left[U^f(\boldsymbol{x}) + U^\omega(\boldsymbol{x}) \right]_{\boldsymbol{x} \in \partial V(t)} \oint_{\partial V(t)} \boldsymbol{n}\, \mathrm{d}A \equiv \boldsymbol{0}, \end{aligned} \tag{4.10}$$

because the directed surface integral over a closed continuous surface always vanishes. Finally, the volume integral on the right hand side of Eqn. (4.9) can be solved if we generalize Eqn. $(2.5)_1$ for an arbitrary time with an angular velocity of arbitrary magnitude, $\omega(t)$, but directed exclusively in $\boldsymbol{e}'_3$ direction:

$$-\nabla' U^\omega = -\boldsymbol{\omega} \times (\boldsymbol{\omega} \times \boldsymbol{x}') = \omega^2(t)\, (x'_1 \boldsymbol{e}'_1 + x'_2 \boldsymbol{e}'_2). \tag{4.11}$$

This leads to:

$$-\int_{V'(t)} \nabla' U^\omega(\boldsymbol{x}')\, \mathrm{d}V' = \omega^2(t) \int_{V'(t)} (x'_1 \boldsymbol{e}'_1 + x'_2 \boldsymbol{e}'_2)\, \mathrm{d}V' \equiv \boldsymbol{0}, \tag{4.12}$$

since we assume that the center of the co-moving non-inertial frame is always located within the center of gravity. Hence:

$$\int_{t_\mathrm{I}}^{t_\mathrm{F}} \oint_{\partial V(t)} \boldsymbol{n} \cdot \boldsymbol{\sigma} \, \mathrm{d}A \, \mathrm{d}t \equiv \int_{t_\mathrm{I}}^{t_\mathrm{F}} \oint_{\partial V(t)} \boldsymbol{t} \, \mathrm{d}A \, \mathrm{d}t = \boldsymbol{0}. \tag{4.13}$$

This requires that the sum of all tractive forces, $T = \oint_{\partial V(t)} \boldsymbol{t} \, \mathrm{d}A$, vanishes over the time average, which is also guaranteed if they vanish in every instant, *e.g.*, by applying moment couples to the surface of the Earth. This brings us to the discussion of the global ***balance of moment of momentum*** or, since we assume a symmetric stress tensor and no intrinsic spin to Earth particles, of ***total angular momentum***. This equation reads in the inertial frame of reference (see, *e.g.*, [9], pp. 79):

$$\frac{\mathrm{d}}{\mathrm{d}t} \int_{V(t)} \rho \, \boldsymbol{x} \times \boldsymbol{v} \, \mathrm{d}V = \oint_{\partial V(t)} \boldsymbol{x} \times \boldsymbol{t} \, \mathrm{d}A - \int_{V(t)} \rho \, \boldsymbol{x} \times \nabla U^f \left(\boldsymbol{x} \right) \, \mathrm{d}V. \tag{4.14}$$

We start by integrating the left hand side over time and find:

$$\int_{t_\mathrm{I}}^{t_\mathrm{F}} \frac{\mathrm{d}}{\mathrm{d}t} \int_{V(t)} \rho \, \boldsymbol{x} \times \boldsymbol{v} \, \mathrm{d}V \mathrm{d}t = \int_{V(t_\mathrm{F})} \rho \, \boldsymbol{x} \times \boldsymbol{v} \, \mathrm{d}V - \boldsymbol{0}. \tag{4.15}$$

Now we use Eqn. (4.6) and $\boldsymbol{x} = \boldsymbol{x}'$ to rewrite the remaining volume integral w.r.t. the non-inertial frame:

$$\begin{aligned} \int_{V'(t_\mathrm{F})} \rho \, \boldsymbol{x'} \times \left(\boldsymbol{\omega} \times \boldsymbol{x}' \right) \, \mathrm{d}V' &= \boldsymbol{I}' \left(t_\mathrm{F} \right) \cdot \boldsymbol{\omega} \left(t_\mathrm{F} \right), \\ \boldsymbol{I}' \left(t_\mathrm{F} \right) &= \int_{V'(t_\mathrm{F})} \rho \, \left(\boldsymbol{x}' \cdot \boldsymbol{x}' \, \boldsymbol{1} - \boldsymbol{x}' \otimes \boldsymbol{x}' \right) \, \mathrm{d}V, \end{aligned} \tag{4.16}$$

$\boldsymbol{I}' \left(t_\mathrm{F} \right)$ being the inertia tensor at the final time. Note that we did not have to assume incompressibility to obtain this result. Because of $\boldsymbol{\omega} \left(t_\mathrm{F} \right) = \omega_0 \, \boldsymbol{e}_3'$ and by assuming that the co-moving non-inertial system is oriented along the principal axes of the spheroid we may also write for short:

$$\int_{V(t_\mathrm{F})} \rho \, \boldsymbol{x} \times \left(\boldsymbol{\omega} \times \boldsymbol{x}' \right) \, \mathrm{d}V = C \omega_0 \, \boldsymbol{e}_3' \left(t_\mathrm{F} \right). \tag{4.17}$$

This final angular momentum has to be provided somehow. In fact, it is generated by the torque supply on the right hand side of the time-integrated version of Eqn. (4.14). We find:

$$C \omega_0 \, \boldsymbol{e}_3' \left(t_\mathrm{F} \right) = \int_{t_\mathrm{I}}^{t_\mathrm{F}} \oint_{\partial V(t)} \boldsymbol{x} \times \boldsymbol{t} \, \mathrm{d}A \, \mathrm{d}t - \int_{t_\mathrm{I}}^{t_\mathrm{F}} \int_{V(t)} \rho \, \boldsymbol{x} \times \nabla U^f \left(\boldsymbol{x} \right) \, \mathrm{d}V \, \mathrm{d}t. \tag{4.18}$$

The second integrand on the right hand side vanishes as can be shown by using similar constraints and tricks as in context with Eqn. (4.10):

$$\rho_0 \int_{V(t)} \boldsymbol{x} \times \nabla U^f(\boldsymbol{x}) \, \mathrm{d}V = \tag{4.19}$$

$$\rho_0 \left(\oint_{\partial V(t)} \boldsymbol{x} \times \boldsymbol{n} \, \left[U^f(\boldsymbol{x}) + U^\omega(\boldsymbol{x}) \right] \, \mathrm{d}A - \int_{V(t)} \boldsymbol{x}' \times \nabla' U^\omega(\boldsymbol{x}') \, \mathrm{d}V' \right),$$

where Eqn. (2.1) with $\boldsymbol{b} = \boldsymbol{0}$ has been used. We now treat the surface integral as follows:

$$\begin{aligned} &\oint_{\partial V(t)} \boldsymbol{x} \times \boldsymbol{n} \, \left[U^f(\boldsymbol{x}) + U^\omega(\boldsymbol{x}) \right] \, \mathrm{d}A \\ &= \left[U^f(\boldsymbol{x}) + U^\omega(\boldsymbol{x}) \right]_{\boldsymbol{x} \in \partial V(t)} \oint_{\partial V(t)} \boldsymbol{x} \times \boldsymbol{n} \, \mathrm{d}A \equiv \boldsymbol{0} \end{aligned} \tag{4.20}$$

since, for convenience, by referring to a Cartesian unit base, $\boldsymbol{e}_i$, of the inertial system we find:

$$\oint_{\partial V(t)} \boldsymbol{x} \times \boldsymbol{n} \, \mathrm{d}A = \boldsymbol{e}_i \oint_{\partial V(t)} \varepsilon_{ijk} x_j n_k \, \mathrm{d}A = \boldsymbol{e}_i \int_{V(t)} \varepsilon_{ijk} \frac{\partial x_j}{\partial x_k} \, \mathrm{d}V = \tag{4.21}$$

$$\boldsymbol{e}_i \int_{V(t)} \varepsilon_{ijk} \delta_{jk} \, \mathrm{d}V = \boldsymbol{e}_i \int_{V(t)} \varepsilon_{ikk} \, \mathrm{d}V \equiv \boldsymbol{0}.$$

For the remaining volume integral of Eqn. (4.20) we may write this time by assigning the Cartesian unit base of the non-inertial system to the principal axes:

$$\int_{V(t)} \boldsymbol{x}' \times \nabla' U^\omega(\boldsymbol{x}') \, \mathrm{d}V' = \int_{V(t)} \boldsymbol{x}' \times \left[\boldsymbol{\omega} \times (\boldsymbol{\omega} \times \boldsymbol{x}') \right] \, \mathrm{d}V' = \tag{4.22}$$

$$-\omega^2(t) \, \left[\boldsymbol{e}_1' \int_{V(t)} x_2' x_3' \, \mathrm{d}V' - \boldsymbol{e}_2' \int_{V(t)} x_1' x_3' \, \mathrm{d}V' \right] \equiv \boldsymbol{0}.$$

In summary, we have made use of incompressibility, the slow process assumption leading to equipotential surfaces, Gauss' theorem, an angular velocity vector always pointing in $\boldsymbol{e}_3'$ direction, and referred to the principal axes system of the co-moving non-inertial system, in which the deviatoric parts of the inertia tensor vanish. Thus, we conclude that under such circumstances:

$$C\omega_0 \, \boldsymbol{e}_3'(t_\mathrm{F}) = \int_{t_\mathrm{I}}^{t_\mathrm{F}} \oint_{\partial V(t)} \boldsymbol{x} \times \boldsymbol{t} \, \mathrm{d}A \, \mathrm{d}t. \tag{4.23}$$

We conclude that the tractions on the surface have to be applied suitably, such that in the time average only an applied torque in $\boldsymbol{e}_3'$ prevails. We now finally

turn to the total energy balance, also formulated for the inertial system (*cf.*, *e.g.*, [9], pp. 75):

$$\begin{aligned}&\frac{\mathrm{d}}{\mathrm{d}t}\int_{V(t)}\rho\,\left(u+\tfrac{1}{2}\boldsymbol{v}^2\right)\,\mathrm{d}V\\&=-\oint_{\partial V(t)}\boldsymbol{n}\cdot(\boldsymbol{q}-\boldsymbol{\sigma}\cdot\boldsymbol{v})\,\mathrm{d}A+\int_{V(t)}\rho\,\left(-\nabla U^f\cdot\boldsymbol{v}+r\right)\,\mathrm{d}V.\end{aligned}\quad(4.24)$$

For the duration of the whole process, *i.e.*, (I) → (I*) → (F), we assume that the outer surface of the Earth is adiabatically sealed, *i.e.*, $q=\mathbf{0}$ on $\partial V\,(t)$, and that there is no radiation, $r=0$. Moreover, for the specific internal energy, u, we use a constitutive equation of the Dulong-Petit-type, *i.e.*, $u=cT+u_0$, with a specific heat c. We also require isothermal processing, $T=\text{const}$. Thus, since mass is conserved, the internal energy part of the time-integrated version of Eqn. (4.24) drops out completely in both stages and the following result is obtained:

$$\begin{aligned}&\int_{V(t_{\mathrm{I}^*})}\tfrac{1}{2}\rho\,\boldsymbol{v}^2\,\mathrm{d}V=\int_{t_{\mathrm{I}}}^{t_{\mathrm{I}^*}}\oint_{\partial V(t)}\boldsymbol{n}\cdot\boldsymbol{\sigma}\cdot\boldsymbol{v}\,\mathrm{d}A\,\mathrm{d}t-\int_{t_{\mathrm{I}}}^{t_{\mathrm{I}^*}}\int_{V(t)}\rho\,\nabla U^f\cdot\boldsymbol{v}\,\mathrm{d}V\,\mathrm{d}t,\\&\int_{V(t_{\mathrm{F}})}\tfrac{1}{2}\rho\,\boldsymbol{v}^2\,\mathrm{d}V-\int_{V(t_{\mathrm{I}^*})}\tfrac{1}{2}\rho\,\boldsymbol{v}^2\,\mathrm{d}V=\\&\int_{t_{\mathrm{I}^*}}^{t_{\mathrm{F}}}\oint_{\partial V(t)}\boldsymbol{n}\cdot\boldsymbol{\sigma}\cdot\boldsymbol{v}\,\mathrm{d}A\,\mathrm{d}t-\int_{t_{\mathrm{I}^*}}^{t_{\mathrm{F}}}\int_{V(t)}\rho\,\nabla U^f\cdot\boldsymbol{v}\,\mathrm{d}V\,\mathrm{d}t.\end{aligned}\quad(4.25)$$

We evaluate the integrals on the left hand side by using Eqn. (4.6):

$$\int_{V(t_{\mathrm{I}^*})}\tfrac{1}{2}\rho\,\boldsymbol{v}^2\,\mathrm{d}V=\tfrac{1}{2}\omega_0^2\int_{V'(t_{\mathrm{I}^*})}\rho\,\left(x_1'^2+x_2'^2\right)\,\mathrm{d}V'=\tfrac{1}{5}mR^2\omega_0^2,\quad(4.26)$$

$$\int_{V(t_{\mathrm{F}})}\tfrac{1}{2}\rho\,\boldsymbol{v}^2\,\mathrm{d}V=\tfrac{1}{2}\omega_0^2\int_{V'(t_{\mathrm{F}})}\rho\,\left(x_1'^2+x_2'^2\right)\,\mathrm{d}V'\equiv\tfrac{1}{2}C\omega_0^2=\tfrac{1}{5}ma^2\omega_0^2.$$

In the latter formula we refer to the principal axes system of the co-moving non-inertial frame, *i.e.*, specifically to the inertia tensor component denoted by C. Of course, in our model m and a refer to the mass and to the major axis of the Earth spheroid. Moreover, R is related to a by Eqn. (4.3). However, the equations apply to any spinning celestial body, and this is why we have omitted the index E for Earth. Now turn to the remaining volume integrals on the right hand side of Eqn. (4.25). We first note that because we are dealing with a closed system it is possible to write:

$$\int_{V(t)}\rho\,\nabla U^f\cdot\boldsymbol{v}\,\mathrm{d}V=\frac{\mathrm{d}}{\mathrm{d}t}\int_{V(t)}\rho\,U^f\mathrm{d}V.\quad(4.27)$$

Hence:

$$\int_{t_{\mathrm{I}}}^{t_{\mathrm{I}^*}}\int_{V(t)}\rho\,\nabla U^f\cdot\boldsymbol{v}\,\mathrm{d}V\,\mathrm{d}t=\int_{V(t_{\mathrm{I}^*})}\rho\,U^f\mathrm{d}V-\int_{V(t_{\mathrm{I}})}\rho\,U^f\mathrm{d}V\equiv 0,\quad(4.28)$$

$$\int_{t_{\mathrm{I}^*}}^{t_{\mathrm{F}}} \int_{V(t)} \rho \nabla U^f \cdot \boldsymbol{v} \, \mathrm{d}V \, \mathrm{d}t = \int_{V(t_{\mathrm{F}})} \rho U^f \mathrm{d}V - \int_{V(t_{\mathrm{I}^*})} \rho U^f \mathrm{d}V.$$

All integrals can be solved in closed form by using Eqn. (2.7), which can also be specialized to a sphere. If we use Eqn. (4.3) we find:

$$-\int_{t_{\mathrm{I}}}^{t_{\mathrm{I}^*}} \int_{V(t)} \rho \nabla U^f \cdot \boldsymbol{v} \, \mathrm{d}V \, \mathrm{d}t = \tfrac{6}{5} \frac{Gm^2}{a} \left(\frac{\arccos \lambda}{\sqrt{1-\lambda^2}} - \frac{1}{\lambda^{1/3}} \right), \lambda = 1 - f. \quad (4.29)$$

Thus, we arrive at:

$$\tfrac{1}{5} m R^2 \omega_0^2 = W^{\sigma}_{\mathrm{I} \to \mathrm{I}^*}, \frac{2\omega_0^2 a^3 \lambda}{3Gm} = 4 \left(\frac{\arccos \lambda}{\sqrt{1-\lambda^2}} - \frac{1}{\lambda^{1/3}} \right) + \frac{10a}{3Gm^2} W^{\sigma}_{\mathrm{I}^* \to \mathrm{F}} \quad (4.30)$$

with the works done by the surface tractions during the two steps:

$$W^{\sigma}_{\mathrm{I} \to \mathrm{I}^*} = \int_{t_{\mathrm{I}}}^{t_{\mathrm{I}^*}} \oint_{\partial V(t)} \boldsymbol{n} \cdot \boldsymbol{\sigma} \cdot \boldsymbol{v} \, \mathrm{d}A \, \mathrm{d}t, W^{\boldsymbol{\sigma}}_{\mathrm{I}^* \to \mathrm{F}} = \int_{t_{\mathrm{I}^*}}^{t_{\mathrm{F}}} \oint_{\partial V(t)} \boldsymbol{n} \cdot \boldsymbol{\sigma} \cdot \boldsymbol{v} \, \mathrm{d}A \, \mathrm{d}t. \quad (4.31)$$

Note that none of these equations allows us predicting the flattening. The first one merely serves for computing the work required by the tractions to bring the sphere, when treated as a rigid body, up to a constant spinning rate. The second one is more interesting. It allows to assess the work of the tractions, $W^{\sigma}_{\mathrm{I}^* \to \mathrm{F}}$, required for transformation of the spinning body from a sphere into a spheroid, if we only combine it with Eqn. (2.13), into which the experimentally observed flattening values are inserted. The final result reads:

$$\frac{10a}{3Gm^2} W^{\sigma}_{\mathrm{I}^* \to \mathrm{F}} = \frac{4}{\lambda^{1/3}} - \frac{3\lambda^2}{1-\lambda^2} - \frac{\left[4 - \lambda - 2\lambda^2 (2+\lambda)\right] \arccos \lambda}{(1-\lambda^2)^{3/2}}. \quad (4.32)$$

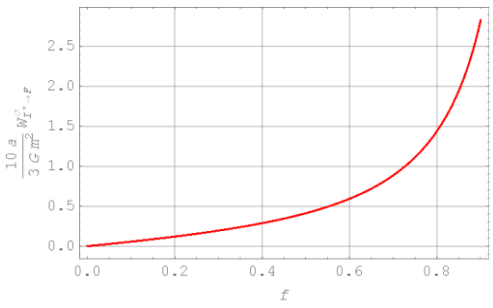

Fig. 4.1: Graphic representation of Eqn. (4.32), allowing to compute the work required for achieving a certain amount of flattening.

Fig. 4.1 shows the behavior of this function. The work increases for increasing flattening. This is what we expect since matter is moved apart against its gravitational pull.

We may conclude that the global balances do not reveal anything regarding the flattening, in contrast to what we might have suspected.

5 Conclusions and outlook

In this paper we have provided a rather comprehensive analysis of the flattening phenomenon. We started from its history, which is almost 400 years old. Then two constitutive models were discussed extensively. In the first model, the spinning celestial body was treated as an incompressible fluid and, in the second one, as a linear-elastic Hookean material. The corresponding boundary value problems were defined, and the local field equations were solved in closed form. Both models were numerically evaluated for terrestrial planets, gas giants, moons and asteroids, as well as stars. The predictions for the corresponding flattening values were compared to experimental observations. Reasons for discrepancies were discussed. It is particularly noteworthy that the linear-elastic solution is not valid for larger telluric planets including Earth. A non-linear solution for large deformations needs to be found in this case. However, this is left to future research.

Moreover, the global balances of mass, momentum, angular momentum, and energy were integrated over time. Explicit closed-form expressions for the work required to produce a spinning, flattened celestial object were, to our knowledge, derived for the first time.

In all of these investigations a homogeneous mass density was a prerequisite. So far, an onion-layered type of Earth model for the flattening has neither been formulated nor analyzed. In principle the Hookean approach presented in Section 3 would allow to study such a situation by adding certain transition conditions between the layers. In fact, it would even be possible to combine the linear elastic and the fluid model by determining the coefficients of the Legendre series appropriately. However, such a solution would definitely involve a considerable amount of additional algebra and, in the end, most likely lead to rather cumbersome expressions. Therefore, it seems justified to perform a fully numerical analysis from the very beginning on, for example by discretizing the Earth using finite elements. This way not only the effects of a heterogeneous mass density distribution could be investigated, but also the impact of constitutive equations beyond linear elasticity. All of this is left to future investigations.

References

[1] Koyré, A., Cohen, I.B., Whitman, A. Isaac Newton's Philosophiae Naturalis Principia Mathematica, the third edition (1726) with variant readings, Volume I / II, Cambridge at the University Press 1972.

[2] Chandrasekhar, S. Newton's Principia for the common reader, Clarendon Press Oxford 1995.

[3] Fitzpatrick, R. Fluid mechanics, http://farside.ph.utexas.edu/teaching /336L/Fluid.pdf.

[4] Thomson, W., Tait, P.G., Treatise on natural philosophy, Part II, Cambridge at the University Press, 1912.

[5] Klein, F. Sommerfeld, A., The theory of the top, Volume III, Perturbations, astronomical and geophysical applications, translated by R.J. Nagem and G. Sandri, Birkhuser, 2012.

[6] Stacey, F.D., Davis, P.M., Physics of the Earth, 4th Edition, Cambridge University Press, 2008, Chapter 7.

[7] http://en.wikipedia.org/wiki/Earth, http://en.wikipedia.org/wiki/Sidereal_time#Sidereal_time_and_solar_time

[8] http://nssdc.gsfc.nasa.gov/planetary/factsheet

[9] Müller, W.H., An expedition to continuum theory, Springer Verlag, Dordrecht 2014.

[10] Fitzpatrick, R., Newtonian dynamics, ebookbrowse, http://ebookbrowsee. net/richard-fitzpatrick-newtonian-dynamics-pdf-d252403265.

[11] Bretagnon, P., Rocher, P., Simon, J.L., Theory of the rotation of the rigid Earth, Astron. Astrophys., 319, pp. 305-317, 1997.

[12] Bursa, M., Current estimates of the Earth's principal moments of inertia, Studia geoph. et geod., 36, pp. 109-115, 1992.

[13] Munk, W.H., MacDonald, G.J.F., The rotation of the Earth, A Geophysical discussion, Cambridge University Press, reprint with corrections, 1975, Chapters 6 and 10.

[14] Maclaurin, C., A treatise on fluxions in two volumes, Volume I., Printed by T.W. and T. Ruddimans, Edinburgh, 1742.

[15] http://www.encyclopediaofmath.org/index.php/Spherical_coordinates

[16] Rozelot, J.-P., Neiner, C., The rotation of sun and stars, Lect. Notes Phys. 765, Springer, Berlin Heidelberg, 2009.

[17] Dziewonski, A.M., Anderson, D.L., Preliminary reference Earth model, Physics of the Earth and Planetary Interiors, 25, pp. 297-356, 1981.

[18] Miles, B., Ramsey, W.H., On the internal structure of Jupiter and Saturn, Monthly Notices of the Royal Astronomical Society, 112, pp. 234-243, 1952.

[19] Blanch, G., Lowan, A.N., Marshak, R.E., Bethe, H.A., The internal temperature-density distribution of the Sun, Astrophysical Journal, 94, pp. 37-45.

[20] Turcotte, D.L., Schubert, G., Geodynamics, Cambridge University Press, 2^{nd} Edition, 2002.

[21] Thomas, P.C., Davies, M.E., Colvin, T.R., Oberst, J., Schuster, P., Neukum, G., Carr, M.H., McEwen, A., Schubert, G., Belton, M.J.S., The shape of Io from Galileo limb measurements, Icarus, 135(1), pp. 175-180, 1998.

[22] Van Hools, T., Rambaux, N., Karatekin, ., Dehant, V., Rivoldini, A., The librations, shape, and icy shell of Europa, Icarus, 195, pp. 386–399, 2008.

[23] Anderson, J.D., Jacobson, R.A., Lau, E.L., Moore, W.B., Olsen, O., Schubert, G., Thomas, P.C., Shape, Mean radius, gravity field and interior structure of Ganymede, American Astronomical Society, DPS Meeting #33, #35.09; Bulletin of the American Astronomical Society, 33, pg. 1101, 2001.

[24] Anderson, J.D., Jacobson, R.A., McElratha, T.P., Moore, W.B., Schubert, G., Thomas, P.C., Shape, mean radius, gravity field, and interior structure of Callisto, Icarus, 153(1), pp. 157-161, 2001.

[25] Zebker, H.A., Stiles, B., Hensley, S., Lorenz, R., Kirk, R.L., Lunine, J., Size and shape of Saturn's moon Titan, Science, 324(5929), pp. 921-923, 2009.

[26] Hiramatsu, Y., Oka, Y., Determination of the tensile strength of rock by a compression test of an irregular piece, Int. J. Rock. Min. Sci., 3, pp. 89-99.

[27] http://en.wikipedia.org/wiki/Moon,
http://en.wikipedia.org/wiki/Io_%28moon%29,
http://en.wikipedia.org/wiki/Europa_%28moon%29,
http://en.wikipedia.org/wiki/Ganymede_%28moon%29,
http://en.wikipedia.org/wiki/Callisto_%28moon%29,
http://en.wikipedia.org/wiki/Titan_%28moon%29

[28] Lee, W.H.K., Kanamori, H., Jennings, P., Kisslinger, C., International handbook of earthquake & engineering seismology, Part A, Academic Press, 2002.

Previous Issues

1. **W.-L. Schulze**. *Pseudo-differential Calculus and Applications to Non-smooth Configurations.* Volume 1, 2000, 136 p.
2. **S. Camiz.** *Exploratory 2- and 3-way Data Analisys and Applications.* Volume 2, 2001, 44 p.
3. **G. Jaiani**. *Theory of Cusped Euler-Bernoulli Beams and Kirchhoff-Love Plates*. Volume 3, 2002, 129 p.
4. **G. Jaiani, S. Kharibegashvili, D. Natroshvili, W.L. Wendland**. *Hierarchical Models for Cusped Plates and Beams.* Volume 4, 2003, 121 p.
5. **A. Bernardini, G. Bretti, P.E. Ricci.** *Laguerre-type Exponentials, Multidimensional Special Polynomials and Applications.* Volume 5, 2004, 28 p.
6. **Ts. Gabeskiria, G. Jaiani, J. Antidze, G. Datashvili.** *English-Georgian-Russian-German-French-Italian Glossary of Mathematical Terms.* Volume 6, 2005, 228 p.
7. **J. Rogava, M. Tsiklauri**. *High Order Accuracy Decomposition Schemes for Evolution Problem.* Volume 7, 2006, 164 p.
8. Volume 8, 2007 **was dedicated to the Centenary of Ilia Vekua.**

   It contains the following articles:

   - **R.P. Gilbert, G.V. Jaiani.** *Ilia Vekua's Centenary*
   - **H. Begehr, T. Vaitekhovich.** *Complex Partial Differential Equations in a Manner of I.N. Vekua.* pp. 15-26
   - **B.-W. Schulze.** *Operators on Configurations with Singular Geometry.* pp. 27-42
   - **V. Kokilashvili, V. Paatashvili.** *On the Riemann-Hilbert Problem in Weighted Classes of Cauchy Type Integrals with Density from* $L^{P(\cdot)}(\Gamma)$. pp. 43-52
   - **Tavkhelidze.** *Classification of a Wide Set of Geometric Figures.* pp. 53-61
9. **N. Chinchaladze**. *On Some Nonclassical Problems for Differential Equations and Their Applications to the Theory of Cusped Prismatic Shells*. Volume 9, 2008, 92 p.
10. **D. Caratelli, B. Germano, J. Gielis, M.X. He, P. Natalini, P.E. Ricci**. *Fourier Solution of the Dirichlet Problem for the Laplace and Helmholtz Equations in Starlike Domains*. Volume 10, 2009, 64 p.
11. **A. Cialdea.** *The* L^P*–Dissipativity of Partial Defferential Operators.* Volume 11, 2010, 94 p.
12. **D. Natroshvili.** *Mathematical Problems of Thermo-Electro-Magneto-Elasticity*. Volume 12, 2011, 128 p.
13. **G. Akhalaia, G. Giorgadze, V. Jikia, N. Kaldani, G. Makatsaria, N. Manjavidze.** *Elliptic Systems on Riemann Surface*. Volume 13, 2012, 155 p.
14. **I. Vekua.** *On Metaharmonic Functions.* Volume 14, 2013, 62 p.

Information for the Authors

1. Papers written in English should be submitted as tex and PDF files via email to the managing editor

Dr. Natalia Chinchaladze
I.Vekua Institute of Applied Mathematics
of Tbilisi State University,
2, University st.
Tbilisi 0186
Georgia
e-mail: chinchaladze@gmail.com

2. Papers should be prepared in any standard version of TeX (i.e. plain, LaTeX, AMS-(La)Tex)

3. Letter's size and intervals between lines should be 12 pt, with a printed text area of 140mm x 225mm on a page.

4. Manuscripts should be compiled in the following order: title page; abstract; keywords; main text; acknowledgments; appendices (as appropriate); references; table(s) with caption(s) (on individual pages); figure caption(s) (as a list).

5. Abstracts of 100-150 words are required for all papers submitted.

6. Each paper should have 3-6 keywords. In addition to keywords, authors are encouraged to provide 2-6 AMS 2010 Mathematics Subject Classification codes.

7. Section headings should be concise and numbered sequentially, using a decimal system for subsections.

8. All the authors of a paper should include their full names, affiliations, postal addresses, telephone and fax numbers and email addresses on the cover page of the manuscript. One author should be identified as the Corresponding Author.

9. The decision on the acceptance is taken after a peer-reviewing procedure.

10. Authors submit their papers on the condition that they have not been published previously and are not under consideration for publication elsewhere.

0179 თბილისი, ი. ჭავჭავაძის გამზირი 1
1 Ilia Chavchavadze Avenue, Tbilisi 0179
tel 995 (32) 225 14 32, 995 (32) 225 27 36
www.press.tsu.edu.ge